Synthesis of Benzo-Fused Benzodiazepines Employed as Probes of the Agonist Pharmacophore of Benzodiazepine Receptors

Weijiang Zhang,† Konrad F. Koehler,§ Bradford Harris,‡ Phil Skolnick,‡ and James M. Cook*,†

Department of Chemistry, University of Wisconsin—Milwaukee, Milwaukee, Wisconsin 53201, Istituto di Ricerche di Biologia Moleculare P. Angeletti (IRBM), via Pontina Km 30,600; 00040 Pomezia (Roma), Italy, and Laboratory of Neuroscience, NIDDK, National Institutes of Health, Bethesda, Maryland 20892

Received October 20, 1993•

The synthesis and *in vitro* evaluation of benzo-fused benzodiazepines **1–6** are described. These "molecular yardsticks" were employed to probe the spatial dimensions of the lipophilic pocket L_2 in the benzodiazepine receptor (BzR) cleft and to determine the effect of occupation of L_2 with respect to agonist activity. Of the new analogs synthesized, the 7,8-benzo-fused benzodiazepine **6** displayed moderately high affinity for the BzR (IC_{50} = 55 nM) and exhibited both anticonvulsant ($ED_{50} \approx 15$ mg/kg) and muscle relaxant ($ED_{50} \approx 15$ mg/kg) activity. As expected, **2** and **4** interacted with the repulsive regions of interaction, S_1 and S_2, and exhibited low affinities for BzR. The rigid nature of these molecular yardsticks (especially **6**, Figure 7) has been employed to probe the depth of L_2. Moreover, in the case of **6** full occupation of L_2 has resulted in an increase in the muscle relaxant effect at the expense of the anticonvulsant/anxiolytic effect.

Introduction

Since the introduction of Librium in 1960[1] and the subsequent discovery of its mode of action[1] *via* γ-aminobutyric acid receptors ($GABA_A$ R), the benzodiazepines have enjoyed widespread use rivaled by few other classes of compounds. The $GABA_A$ receptors are a heterooligomeric group of ligand-gated ion channels that constitute the major inhibitory neurotransmitter system in the mammalian central nervous system (CNS).[2] The identification of multiple α, β, and γ subunits[3-5] is consistent with pharmacological evidence of multiple $GABA_A$ receptor isoforms in the CNS.[6] Molecular biological studies have established that expression of either two (α, γ) or three (α, β, γ) subunits are necessary to constitute a functional receptor which mimics many of the pharmacological, biochemical, and electrophysiological properties of native receptors.[7-9] However, neither the stoichiometry nor the composition of native $GABA_A$ receptors in the CNS has been evinced.

SAR data available for a number of structurally diverse ligands has led to the development of several different models of the benzodiazepine receptor (BzR) pharmacophore.[10-17] A common feature of these models attempts to explain ligand efficacy (that is, GABA positive, GABA neutral, GABA negative) as a function of ligand–receptor interaction at the molecular level. For example, on the basis of the *in vitro* and *in vivo* profiles of pyridodiindoles (2-methoxy-7,12-dihydropyridodiindole, 2-chloro-7,12-dihydropyridodiindole), β-carbolines (βCCM, βCCE, DMCM), pyrazoloquinolinones (CGS-8216), and the thienylpyrazoloquinolinones (TPQ), as well as computer modeling studies [alignment rule], a model of the pharmacophore for inverse agonists/antagonists was developed in our laboratory (Figure 1).[18,19]

Recently, a preliminary model for the agonist pharmacophore[20,21] has been designed *via* a chemical- and computer-assisted approach analogous to that employed for inverse agonists (Figure 2). Three points were employed initially for the least-squares fitting of each ligand, and these pharmacophoric descriptors were termed L_1, H_1, and H_2 (Figure 2).[20] In addition, lipophilic area L_2 which represents the region of overlap of the substituents (Cl, OCH_3, Me, Et) on the D rings of the pyrazoloquinolinones (CGS) and the thienylpyrazoloquinolinones (TPQ), respectively, as well as the Cl and NO_2 groups at position 7 of the typical 1,4-benzodiazepines (diazepam, etc.), has been defined. Interaction at H_1, H_2, L_1, and L_2 is critical for potent agonist activity. In the case of the 1,4-benzodiazepines (flunitrazepam, diazepam, etc.), the 5-phenyl group (C ring) interacts with a third lipophilic area termed L_3. An area of negative steric interaction has been termed S_1 and has been described in a previous report.[20,21]

To account for the bidirectional effect of GABA on agonist and inverse agonist binding to BzR, Skolnick *et al.*[22,23] postulated a domain hypothesis for ligand interaction wherein both classes of compounds were proposed to bind to different areas of the same binding region. Consistent with this hypothesis, the pharmacophoric descriptors H_1 and L_1 are common to the site for both inverse agonists and agonists; however, the pharmacophoric descriptors required for agonist (H_1, H_2, L_1, L_2, and/or L_3) and inverse agonist (H_1, A_2, and L_1) activity are clearly different (see Figures 1 and 2).[24] The overlap of the two pharmacophores depicted in Figure 3 represented as the total included volume (agonists = green, inverse agonists = violet) provides a better representation of the binding site at BzR especially with regard to ligand efficacy *in vivo* (Figure 3).

Recent evidence suggests that full occupation of L_3 by the phenyl ring (C-6) of ZK-93423 resulted in a full agonist spectrum of activity (anxiolytic, anticonvulsant, muscle relaxant, sedative-hypnotic),[20,21,25] while partial occupation of this same region with a propyl group (C-6) resulted in an anxiolytic/anticonvulsant [6-(propyloxy)-4-(methoxymethyl)-β-carboline acid ethyl ester, 6PBC] response devoid of muscle-relaxant activity, a so-called partial agonist profile.[21] Clearly much work must be carried out to confirm this hypothesis. In order to determine the size of lipophilic region L_2 and the effect of occupation of L_2

† University of Wisconsin—Milwaukee.
§ Istituto di Ricerche di Biologia Moleculare P. Angeletti (IRBM).
‡ National Institutes of Health.
• Abstract published in *Advance ACS Abstracts*, February 15, 1994.

0022-2623/94/1837-0745$04.50/0

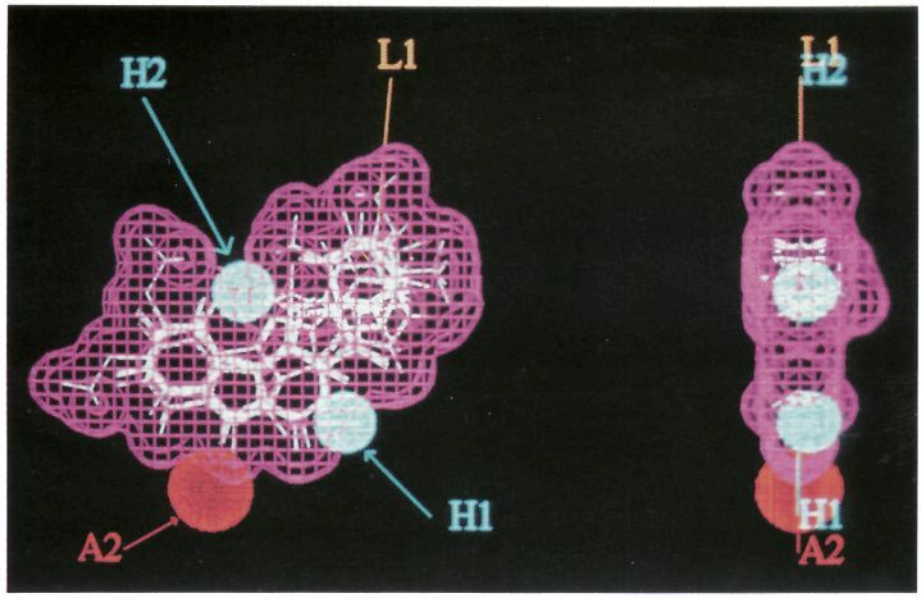

Figure 1. The superposition of 12 inverse agonist ligands and the included volume analysis of the inverse agonist pharmacophore at the benzodiazepine binding site (βCCE, DMCM, 3-ethoxy-β-carboline, 3-propionyl-β-carboline, CGS-8216, 7,12-dihydropyrido-[3,2-*b*:5,4-*b*′]diindole, 2-methoxy-7,12-dihydroxypyrido[3,2-*b*:5,4-*b*′]diindole, 2-thienylpyrazolo[3,4-*c*]quinolin-3-one, 2-(4′-methylthienyl)pyrazolo[3,4-*c*]quinolin-3-one, 3-thienylpyrazolo[3,4-*c*]quinolin-3-one, 3-(5′-methylthienyl)pyrazolo[3,4-*c*]quinolin-3-one, and 3-(4′-methylthienyl)pyrazolo[3,4-*c*]quinolin-3-one). The inverse agonist pharmacophoric descriptors H_1 and H2 represent hydrogen bond donor sites on the protein; A_2 represents a hydrogen bond acceptor site on the protein; L_1 represents a lipophilic pocket. The illustration on the right side of the picture (orthographic stereoview) originates from rotation of the pharmacophore 90° to the left.

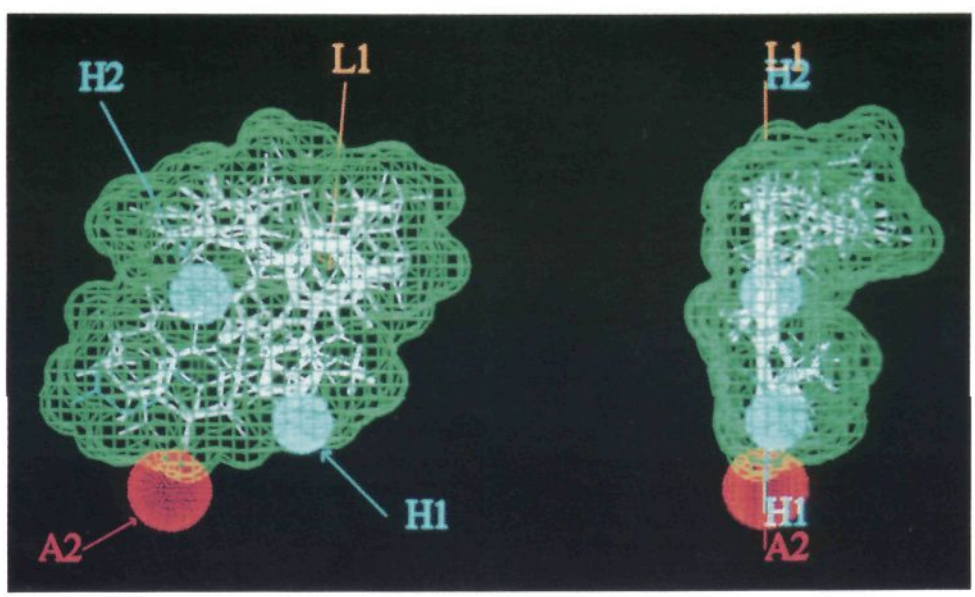

Figure 2. The superposition of 24 different agonist ligands representing 70 different agonists and the included volume analysis of the agonist pharmacophore at the benzodiazepine receptor binding site (diazepam, brotizolam, delorazepam, midazolam, triazolam, norflunitrazepam, 7-aminoflurazepam, 7,2′-dichloro-thieno[2,3–*e*][1,4]benzodiazepine, 1-methyl-8-chloro-2′-fluoro-*s*-triazolo[4,3-*a*]-[1,4]benzodiazepine, 2,9-dichloropyrimido[5,4-*d*][2]benzazepine, 4-chloro-5-(dibutylamino)-3-aryl-1,2,4-triazolo[3,4-*a*]phthalazine, 2-benzoyl-5-methoxy-7-ethylimidazo[1,2-*a*]quinoline, 2-benzoyl-5-(methylthio)-6-methyl-7-ethylimidazo[1,2-*c*]pyrimidine, 2-(4′-chlorophenyl)pyrazolo[3,4-*c*]quinolin-3-one, 2-(5′-methylthienyl)pyrazolo[3,4-*c*]quinolin-3-one, 2-(5′-ethylthienyl)pyrazolo[3,4-*c*]quinolin-3-one, 2-(5′-butylthienyl)pyrazolo[3,4-*c*]quinolin-3-one, 2-(4′,5′-dimethylthienyl)pyrazolo[3,4-*c*]quinolin-3-one, 3-(5′-butylthienyl)-pyrazolo[3,4-*c*]quinolin-3-one, 6-(benzyloxy)-4-(methoxymethyl)-β-carboline-3-carboxylic acid ethyl ester, 5-(benzyloxy)-4-(methoxymethyl)-β-carboline-3-carboxylic acid ethyl ester, 6-(benzyloxy)-4-(methoxymethyl)-β-carboline-3-carboxylic acid isopropyl ester, 6-(propyloxy)-4-(methoxymethyl)-β-carboline-3-carboxylic acid ethyl ester). The agonist pharmacophoric descriptors H_1 and H_2 represent hydrogen bond donor sites on the protein; L_1, L_2, and L_3 represent lipophilic pockets in the protein. The illustration on the right side of the picture (orthographic stereoview) originates from rotation of the pharmacophore 90° to the left.

on agonist activity, a series of benzo-fused benzodiazepines has been designed (Figure 4).

The use of "molecular yardsticks" in the diindole series to define the boundary of the repulsive region S_1 was recently reported.[24,26] Potential 7,8-disubstituted molecular yardsticks in the 1,4-benzodiazepine series are depicted in Figure 5. The complementary probes in the 6,7- and 8,9-benzo-fused systems are illustrated here only for the benzo-fused benzodiazepines **1** and **2** (Figure 4). Molecular yardsticks (benzo-fused rings) employed here

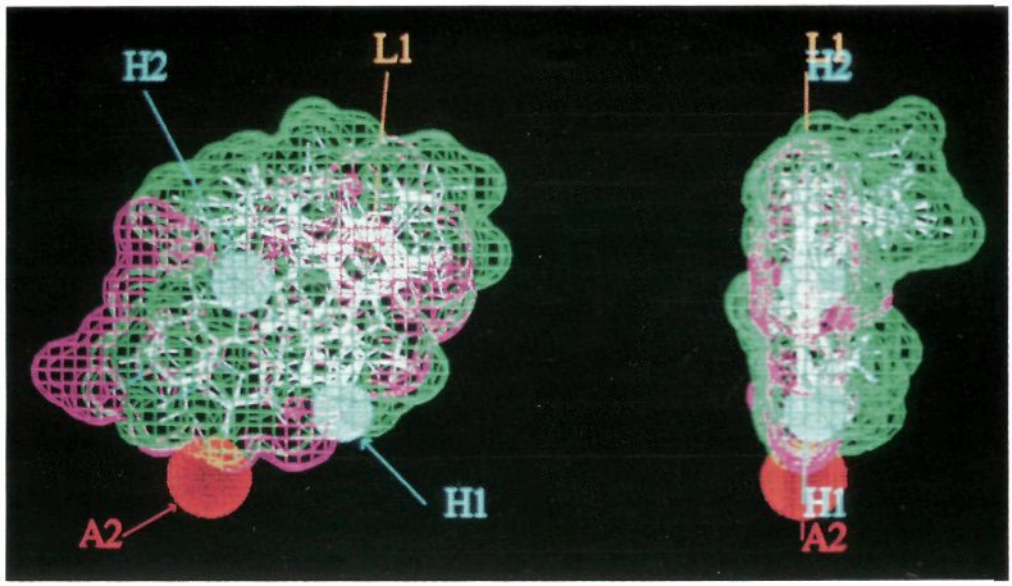

Figure 3. The included volume of agonist ligands is shown in green while the included volume of inverse agonists is represented in violet. The illustration on the right side of the picture (orthographic stereview) originates from rotation of the pharmacophore 90° to the left.

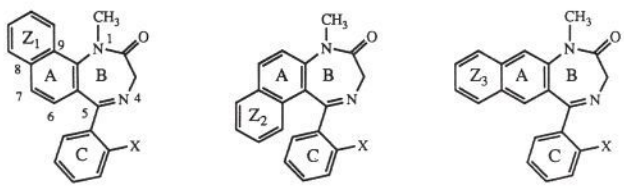

1 X=H
4 X=F

2 X=H
5 X=F

3 X=H
6 X=F

Figure 4. Benzo-fused 1,4-benzodiazepines.

represent rigid probes to define the dimensions of the lipophilic pockets of the BzR in the absence of complications introduced by rotational freedom, simplifying the molecular modeling. Even in the cases of the 7,8-dimethyl, 7,8-di-*tert*-butyl, or 7,8-bis(trihalo) analogues rotational freedom of the symmetrically substituted carbon atoms does not complicate the molecular modeling.[27]

The SAR of the classical 1,4-benzodiazepines (diazepam, flunitrazepam, nitrazepam, etc.) has been extensively reported.[28] It is well documented that substitution of an electron-withdrawing group at position 7 (L_2) and a halogen atom at position 2′ (H_2) for a hydrogen atom increases the affinity and efficacy at the BzR in this series. Moreover, the phenyl ring at C(5) of diazepam is also required (L_3) for a full agonist spectrum of activity.[20,21] On the basis of the above SAR, the proposed interaction between the benzo-fused 1,4-benzodiazepine system and the agonist pharmacophore/receptor model is illustrated in two dimensions in Figure 6. All of these ligands contain the required functional groups to form hydrogen bonds at H_1 and H_2 of the receptor protein, as well as fulfill the requirements of L_1 and L_3. As indicated, the linear 7,8-benzo-fused ligand (panel B) should just fit into the region L_2 and bind to the BzR as an agonist, whereas the 8,9-benzo-fused ligand (panel A) would interact in the region of negative steric repulsion (S_1) with little or no affinity at the BzR. The 6,7-benzo-fused ligand (panel C) does not occupy L_2 and should, therefore, exhibit little or no agonist activity. This ligand may elicit weak antagonist activity; however, if the *in vitro* affinities of **2** and **5** are low, this will help to better outline the area S_2. This is defined as a region of negative steric interaction at the boundary between lipophilic pockets L_2 and L_3, as illustrated in Figure 6.

Chemistry

The present series of compounds were prepared in order to better define the dimensions of the proposed lipophilic pocket (L_2) and the effect of its occupation on the profile of *in vivo* activity. The benzo-fused 1,4-benzodiazepines **1–3** were synthesized by methods outlined in the review by Fryer.[12] In this sequence, the preparation of the necessary α-aminobenzophenones **7–9** is required and is illustrated in Scheme 1.[29] Conversion of 1-nitronaphthalene **10** into 1-amino-2-naphthonitrile **12** was accomplished via the method of Tomioka *et al.*[30] This novel transformation constitutes a one-pot sequence to convert an *arylnitro compound into an ortho-substituted aminoaryl* nitrile. The 1-nitronaphthalene **10** was heated in a mixture of ethyl cyanoacetate, potassium cyanide, and potassium hydroxide for 36 h at 50 °C. This process was followed by hydrolysis as depicted in Scheme 1 to furnish the desired 1-amino-2-naphthalenecarbonitrile (**12**) in 60% yield. The 2-nitro analog **11** was converted into 2-amino-1-naphthalenecarbonitrile (**13**) under conditions analogous to those described above in 56% yield. Regiospecific orthocyanation of the nitronaphthyl derivative with concomitant reduction of the nitro moiety had occurred in the same simple process.

The 1-amino-2-naphthonitrile (**12**) was stirred with 3 equiv of phenylmagnesium bromide, and this was followed by hydrolysis to provide 1-amino-2-benzoylnaphthalene (**7**) in 85% yield. The reaction of 2-amino-1-naphthonitrile (**13**) with 3 equiv of phenylmagnesium bromide in ether was followed by hydrolysis with 6 N aqueous HCl at reflux to furnish 2-amino-1-benzoylnaphthalene (**8**) in 86% yield. The intermediate in this process, an unusually stable imine (C=NH), could not be hydrolyzed in 2 N aqueous HCl (5 h at 30 °C); consequently, more vigorous conditions were required. The 2-amino-3-benzoylnaphthalene derivative **9** was synthesized from commercially available 3-amino-

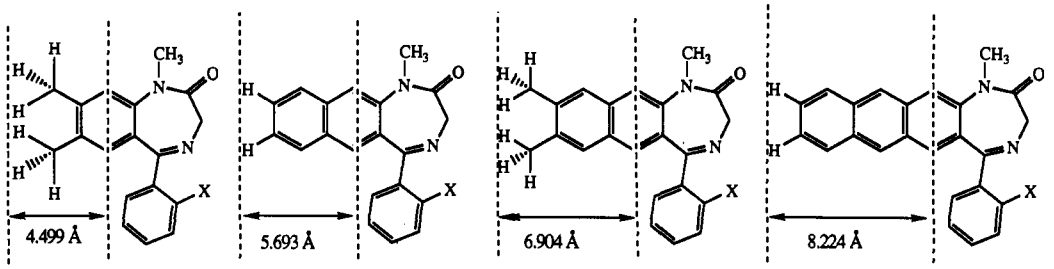

Figure 5. Two-dimensional molecular yardsticks. Distances cited are between the centroid of the benzene ring and the edge of the van der Waals field of the protons.

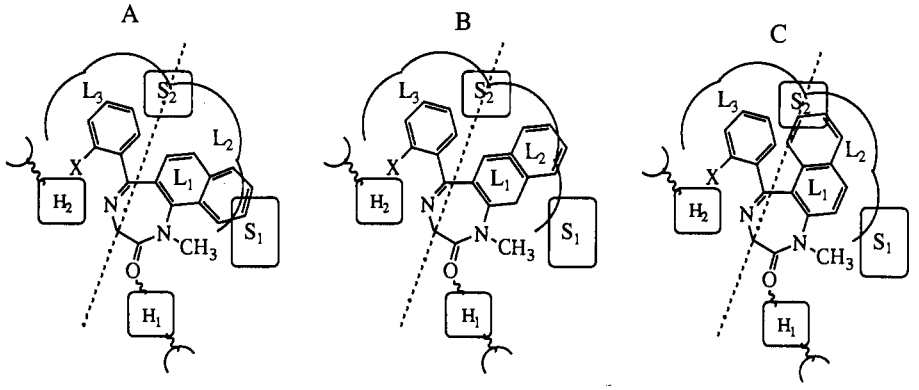

Figure 6. H_1, H_2 are the hydrogen bond donor sites on the receptor protein. L_1, L_2, and L_3, are the lipophilic pockets in the protein at the binding site. S_1 and S_2 are the areas of negative interaction between the ligand and the protein at the binding site.

Scheme 1

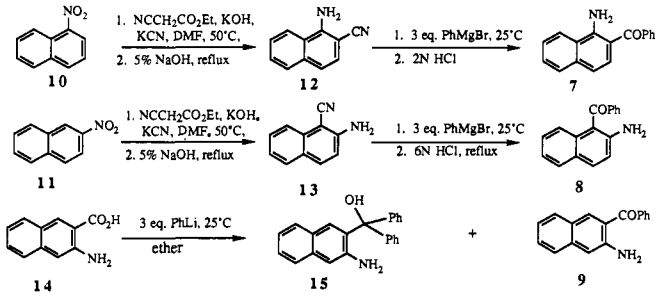

Scheme 2[a]

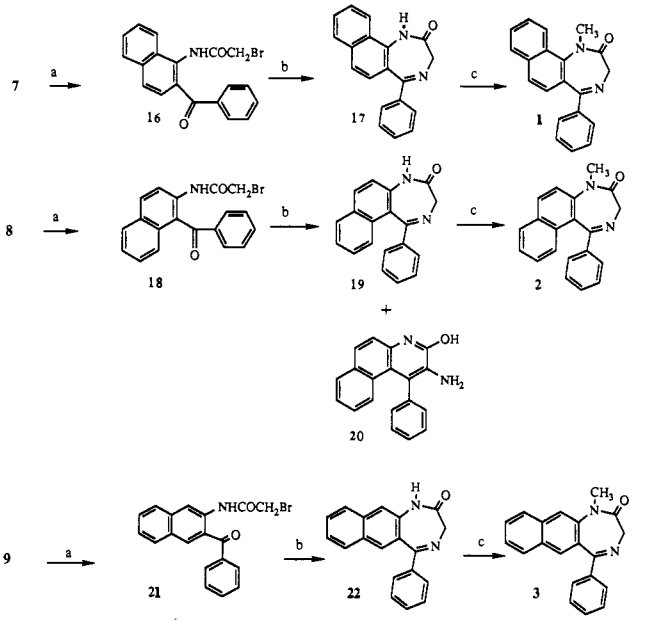

[a] (a) $BrCH_2COBr/NaHCO_3$, 0 °C, $CHCl_3$; (b) NH_3/MeOH reflux; (c) NaH/MeI, DMF.

2-naphthoic acid (**14**). This acid **14** was stirred with 3 equiv of phenyllithium at 25 °C to provide the desired α-aminobenzophenone **9** in 51% yield, accompanied by 10% of the diphenyl tertiary alcohol **15**.

The three α-aminobenzophenones **7–9** were converted into the target benzo-fused benzodiazepines **1–3**, as illustrated in Scheme 2. In brief, acylation of α-aminobenzophenone **7** with 1.1 equiv of bromoacetyl bromide gave the corresponding 1-(*N*-(bromoacetyl)amino)-2-benzoylnaphthalene **16** in 94% yield. A solution of the amide **16** was stirred in a saturated solution of ammonia in methanol at reflux to produce the benzo-fused benzodiazepine derivative 5-phenyl-1,3-dihydronaphtho[1,2-*e*]-[1,4]diazepin-2-one (**17**) in 74% yield. Methylation of **17** with methyl iodide in the presence of sodium hydride gave the desired *N*(1)-methyl-5-phenyl-1,3-dihydronaphtho-[1,2-*e*][1,4]diazepin-2-one (**1**, 87%). Acylation of α-aminobenzophenone **8** with 1.1 equiv of bromoacetyl bromide gave the corresponding 2-(*N*-(bromoacetyl)amino)-1-benzoylnaphthalene **18** in 89% yield. A solution of the amide **18** in methanol was reacted with ammonia to produce the benzo-fused benzodiazepine derivative 5-phenyl-1,3-dihydronaphtho[2,1-*e*][1,4]diazepin-2-one (**19**) in 39% yield and the quinoline byproduct (**20**) in 44% yield. It is believed that in **19** the 5-phenyl ring and the 6,7-fused benzene ring experience a negative steric interaction which retarded the cyclization of **18** to **19**, to the benefit of byproduct **20**. The benzoquinoline **20** would arise from attack of the methylene group of **18** on the ketone, followed by dehydration to form the more stable aromatic quinoline system. Presumably, ammonia has displaced the bromine atom in **18** before this quinoline **20** was formed. Methylation of **19** with methyl iodide in the presence of sodium hydride gave the desired *N*(1)-methyl-5-phenyl-1,3-dihydronaphtho[2,1-*e*][1,4]diazepin-2-one (**2**) in 90% yield. Acylation of α-aminobenzophenone **9** was followed by the amination/cyclization process, as described above, to produce the benzo-fused benzodiazepine derivative 5-phenyl-1,3-dihydronaphtho[2,3-*e*][1,4]diazepin-2-one (**22**) in

Table 1. *In Vitro* IC_{50} Values of New Ligands at the BzR

compd	no.	R	X	IC_{50} (nM)[a]	ref
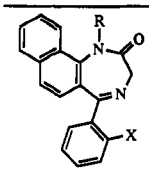	1	CH_3	H	>1000	
	17	H	H	>1000	
	4	CH_3	F	260 ± 25	
	38	H	F	120 ± 20	
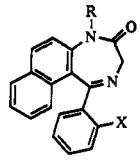	2	CH_3	H	>1000	
	19	H	H	>1000	
	5	CH_3	F	>1000	
	40	H	F	>1000	
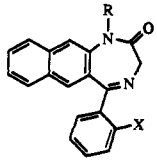	3	CH_3	H	>1000	
	22	H	H	400 ± 30	
	6	CH_3	F	55 ± 2	
	42	H	F	>1000	
ZK-93423				5	25
diazepam				6	24

[a] See the Experimental Section for details.

Scheme 3

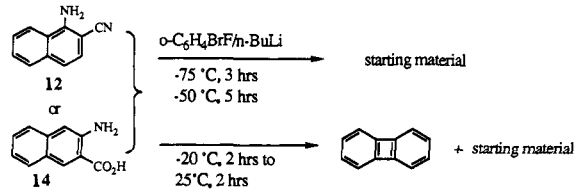

78% yield. Methylation of **22** with methyl iodide in the presence of sodium hydride gave the desired *N*(1)-methyl-5-phenyl-1,3-dihydronaphtho[2,3-*e*][1,4]diazepin-2-one (**3**) in 88% yield.

The three analogs were screened for *in vitro* affinity to benzodiazepine receptor sites on rat cortical membranes, the data from which is depicted in Table 1. As can be seen from the data in Table 1, none of these analogs exhibited potent affinity to BzR. This is not surprising, for examination of the ligand–receptor fit illustrated in Figure 6 for **1–3** indicates that there is little room to spare in the binding site at S_1, L_2, and S_2, respectively. It is known, however, that substitution of fluorine for hydrogen at the 2′-position of the 1,4-benzodiazepines greatly enhances affinity and efficacy at the BzR.[28] This is particularly important with reference to ligands **1–3** for the 2′-fluorine substituent could interact at H_2 in place of N(4), permitting some ligand flexibility (plasticity) in the binding cleft. For this reason attention turned toward the synthesis of benzo-fused ligands **4–6**.

When naphthonitrile **12** or amino acid **14** was reacted (individually) with the anion of *o*-C_6H_4BrF/*n*-BuLi (1:1) [(*o*-fluorophenyl)lithium] at low temperature (−75 °C to −50 °C for 5 h), only starting materials were recovered, respectively. When the temperature was elevated to −30 °C to 25 °C, only starting materials and biphenylene were obtained in reasonable amounts (Scheme 3). The structure of biphenylene was confirmed by comparison of its properties to those of an authentic sample (see the Experimental Section). These results indicated that the nitrile and carboxylate moieties in the two series were not electrophilic enough to react with the anion at low temperature. Unfortunately, at higher temperatures (above −30 °C), the (o-fluorophenyl)lithium underwent

Scheme 4

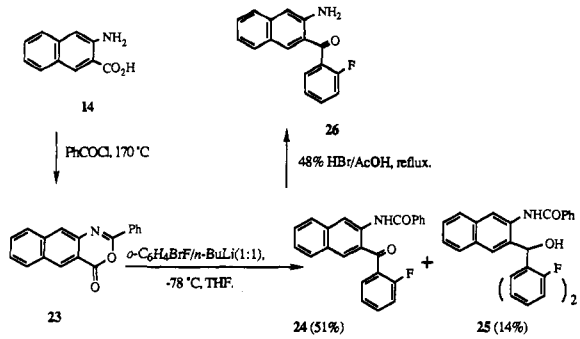

Scheme 5

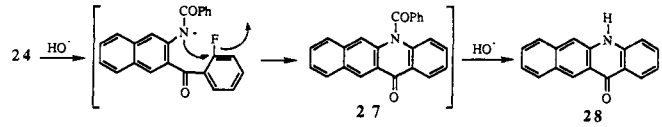

1,2-elimination to form benzyne which dimerized to produce biphenylene (Scheme 3).

In order to circumvent this difficulty, the amino acid **14** was stirred with benzoyl chloride at 170 °C to provide the 2-phenyl-4*H*-naphtho[2,3-*d*]-1,3-oxazin-4-one **23** in 91% yield, according to the procedure of Clemence et al.[31] Treatment of the oxazin-4-one **23** with 1 equiv of (*o*-fluorophenyl)lithium at −78 °C furnished the desired 2′-fluorophenyl ketone **24** in 51% yield,[32] accompanied by 15% of the bis(2′-fluorophenyl) alcohol **25**. Increasing the ratio of the lithium reagent to the naphthoxazinone **23** only increased the yield of the tertiary alcohol **25** (Scheme 4). When the amide **24** was heated in the presence of base (5–10% aqueous NaOH) to effect hydrolysis, the benzoacridone derivative **28** was obtained in more than 80% yield. However, hydrolysis of benzamide **24** under acidic conditions furnished the desired α-amino ketone **26** in 97% yield. The formation of the benzoacridone **28** is interesting and worthy of brief comment. Presumably, the benzamide **24** is converted in base into the anion, as illustrated in Scheme 5. Since the fluorine atom is activated to displacement by the neighboring carbonyl group, the intramolecular nucleophilic attack takes place smoothly and in high yield to furnish acridine derivative **27**. Hydrolysis of the benzamide function *in situ* then led to the 9-oxobenz[*b*]acridine **28**. This sequence may provide a facile route to ring A substituted benzacridones.

In order to prepare the α-amino-2′-fluorobenzophenone required for the synthesis of benzo-fused 1,4-benzodiazepine **4**, 1-amino-2-naphthonitrile **12**, which was readily available by the process of Tomioka *et al.*,[30] was hydrolyzed with 20% NaOH[33] to provide the corresponding 1-amino-2-naphthoic acid **29** in 85% yield. This amino acid **29** was heated with benzoyl chloride at 170 °C to provide the corresponding naphthoxazinone **30** in 91% yield. The naphthoxazinone **30** was stirred with 1 equiv of (*o*-fluorophenyl)lithium at −78 °C to provide the keto amide intermediate **31** (85%) as the only product. This process was followed by hydrolysis (48% HBr/AcOH, Δ) to furnish the desired amine **32** in 95% yield (Scheme 6).

As described earlier, 1-amino-2-naphthonitrile **12** did not react with (o-fluorophenyl)lithium at low temperature. Moreover, all attempts to hydrolyze 2-amino-1-naphthonitrile (**13**) to the corresponding amino acid failed. When **13** was treated under various conditions (20–40% NaOH, Δ; 50–75% H_2SO_4, Δ), the product of decarbox-

Scheme 6

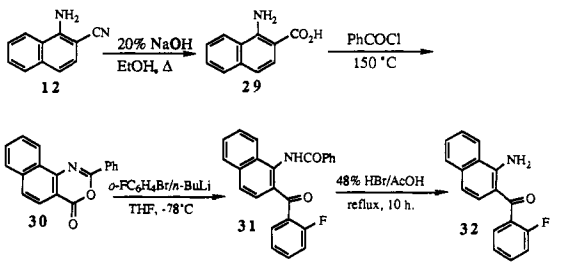

Scheme 7

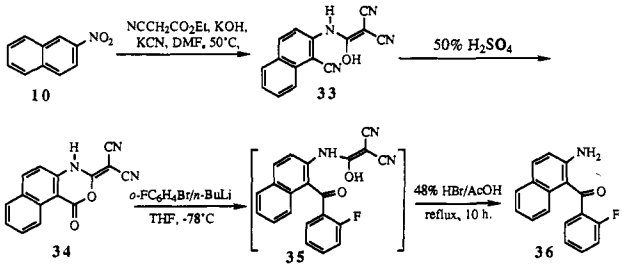

Scheme 8[a]

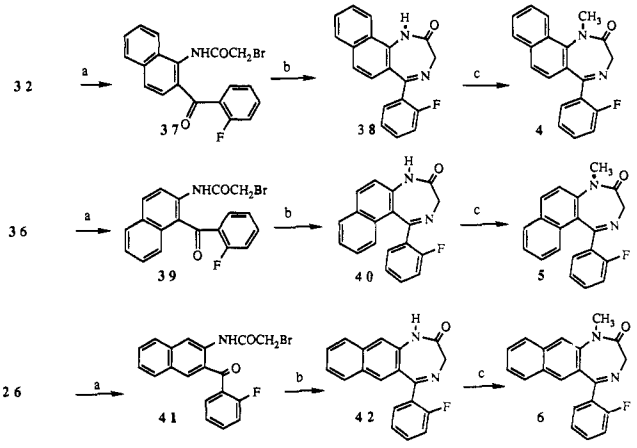

[a] (a) $BrCH_2COBr/NaHCO_3$, 0 °C, $CHCl_3$; (b) NH_3/MeOH reflux; (c) NaH/MeI, DMF.

ylation,[34] 2-aminonaphthalene, was obtained as the only isolable material. Since the starting amino acid related to **13** was not easily obtained, a related intermediate **33** from the process developed by Tomioka *et al.*[35] was prepared (Scheme 7). Hydrolysis of the nitrile **33** in sulfuric acid provided the 2-(dicyanomethylene)naphthoxazinone **34**. This naphthoxazinone was then stirred with 2 equiv of (*o*-fluorophenyl)lithium at −78 °C to generate intermediate **35**, and this step was followed by hydrolysis to furnish the desired fluorine-substituted 1-(2′-fluorobenzoyl)-2-aminonaphthalene **36** in 71% yield.

The syntheses of the 2′-fluorobenzo-fused 1,4-benzodiazepines **4**–**6** were carried out by the methods of Sternbach[36] and Fryer,[12] as illustrated in Scheme 8. Amino ketone **32** was acylated with bromoacetyl bromide to provide the bromo amide **37** in 92% yield. When this amide **37** was heated in a solution of methanol saturated with ammonia the 8,9-benzo-fused 1,4-benzodiazepine **38** was obtained. Methylation under standard conditions, as described above, provided the target *N*(1)-methyl-5-(2′-fluorophenyl)-1,3-dihydronaphtho[1,2-*e*][1,4]diazepin-2-one (**4**) in excellent yield. Conversion of amino ketone **36** into bromo amide **39** was carried out under conditions analogous to those described above. The conversion of the N(1)-H benzodiazepine **40** into the *N*(1)-methyl-5-(2′-fluorophenyl)-1,3-dihydronaphtho[2,1-*e*][1,4]diazepin-2-one (**5**) was executed as indicated in Scheme 8. The 7,8-benzo-fused system, *N*(1)-methyl-5-(2′-fluorophenyl)-1,3-dihydronaphtho[2,3-*e*][1,4]diazepin-2-one (**6**), was prepared in excellent yield by reaction of amino ketone **26** with bromoacetyl bromide, as shown, to generate **41**, followed by amination/cyclization (see **42**) and N(1)-methylation, as illustrated in Scheme 8.

Biological Results and Discussion

The affinities of benzo-fused 1,4-benzodiazepines at BzR were evaluated by previously reported methods.[21,24] Illustrated in Table 1 are the IC_{50} values of these new "molecular yardsticks". The 8,9-benzo-fused ligands **1** and **17** exhibited very little (IC_{50} > 1000 nM) or no affinity to BzR, and this can be attributed to a negative steric interaction with the receptor protein at S_1, which is consistent with the results obtained in the pyridodiindole and pyridoimidazole series.[37] The low affinity of these 8,9-benzo-fused ligands confirms the location of S_1 in the receptor binding cleft, previously reported.[24]

The 6,7-benzfused ligands **2** and **19** have IC_{50} values >1000 nM, supporting the location of S_2 (a negative area of steric interaction between the boundaries of L_2 and L_3). These findings are in agreement with the recent results obtained with the pyridoimidazoles by Martin *et al.*[24,26,37] The low IC_{50} values of the linear 7,8-benzo-fused ligands **3** and **22** indicate only a very weak interaction at the BzR. Again, the rigid phenyl ring must be interacting with the receptor protein (Figure 6), presumably in lipophilic pocket L_2. Because the fit of the 7,8-benzo-fused ring of **3** and **22** in lipophilic pocket L_2 was anticipated as a near acceptable interaction (see Figure 6), an additional modification of these rigid probes was required. It has been well documented, as mentioned above, that substitution of a fluorine atom for hydrogen at the 2′-position of the 1,4-benzodiazepines enhanced the affinity and efficacy of ligands at the BzR; consequently, the 2′-fluoro analogs **4**–**6** were screened. The effect of a fluorine substituent (2′) on the activity of the 8,9-benzo-fused compounds (see **4** and **38**, Table 1) resulted in an increase in potency, while the effect on the 6,7-benzo-fused compounds (see **5** and **40**) was minimal. Substitution of the 2′-hydrogen atom with fluorine in the linear *N*(1)-methyl 7,8-benzo-fused system (see **3**, >1000 nM), however, resulted in a significant enhancement in affinity with the 2′-fluoro ligand **6** exhibiting an IC_{50} value of 55 nM. The increase in binding potency is significant in the context of the agonist pharmacophore/receptor model. The 2′-fluorine substituent is in close proximity to the required hydrogen bonding site H_2 in the proposed ligand binding cleft. It is possible that the required agonist hydrogen bonding interaction at H_2 with **6** now occurs *via* the 2′-fluorine atom rather than the imine nitrogen atom at position 4. This permits **6** to move in the binding site just enough to fit into L_2 without loss of the important interactions at H_1, H_2, L_1, and L_3. This plasticity (flexibility) in the binding cleft is permitted because of the interaction of H_2 with the 2′-fluorine atom.

Because of the high affinity of **6** to the BzR as compared to the activity of the desfluoro analogs, it was chosen for *in vivo* evaluation. Pharmacological studies in mice indicate that *N*(1)-methyl-5-(2′-fluorophenyl)-1,3-dihydronaphtho[2,3-*e*][1,4]diazepin-2-one (**6**) exhibits a full agonist spectrum of activity, analogous to that previously

Table 2. IC_{50} Values and *in Vivo* Activities of 6,7,8,9-Substituted 1,4-Benzodiazepine Ligands at the BzR

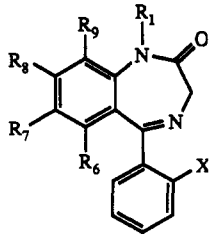

no.	R_6	R_7	R_8	R_9	R_1	X	IC_{50}	activity
43		CH_3	Cl			F	14	0[a]
44		Cl	Cl			F	3.6	+++[a]
45		Cl	Cl		CH_3		40	++
46		CH_3	CH_3					132[b]
47		NO_2		CH_3				8.12[b]
48		Cl		Cl				8[b]
49		CH_3		CH_3				792[b]
50		$CH{=}CH_2$					24	+[a]
51		Ph						781[b]
52	Cl				CH_3	F	150	0[a]
53	Cl						320	0[a]
54		Cl			CH_3		8.1	+++,[a] 1.39[b]

[a] The symbols + to ++++ indicate activities reported in ref 28. [b] Data were obtained from conversion of log (1/C) in ref 38.

reported for diazepam.[21] The ED_{50} for the anticonvulsant effect of **6** was ≈15 mg/kg, and the ED_{50} for the myorelaxant effect was also ≈15 mg/kg. In comparison to diazepam, ligand **6** exhibited a less potent anticonvulsant effect and a comparable ataxic effect. Apparently, full occupation of L_2 has potentiated the muscle relaxant effect of **6** evidently at the expense of the potency of the anticonvulsant/anxiolytic effect. This is somewhat similar to the spectrum of activity elicited by the full agonist ZK 93423 (6-(benzyloxy)-4-(methoxymethyl)-β-carboline-3-carboxylic acid ethyl ester) *vs* the partial agonist 6PBC.[21] In this latter case, partial occupation of L_3 (6PBC) furnished an agent with anxiolytic and anticonvulsant activity devoid of muscle relaxant activity.[21,25] Although speculative, it is reasonable to predict that ligand selectivity and intrinsic activity (efficacy) at different $GABA_A$ receptor isoforms will stem from different interactions in the lipophilic pockets of the BzR(s) receptor binding cleft(s) effected by selective BzR ligands. While it is not known whether transfected cells expressing various $GABA_A$ subunits assemble them with the same stoichiometry as native receptors, future studies with recombinant receptors should provide additional insights into the validity of this hypothesis.

For comparison to **6**, depicted in Table 2 is a list of disubstituted 1,4-benzodiazepines which have been previously reported to bind to the BzR.[28,38] The 7,8-disubstituted ligands **43**, **44**, and **45** exhibit high affinities at the BzR *in vitro* and two of these ligands elicit potent agonist activity. However, ligand **46** (7,8-dimethyl) exhibits only weak agonist activity because it is devoid of the electron-withdrawing group at position 7 required for potent *in vivo* activity of the 1,4-benzodiazepines.[28] However, this 7,8-dimethyl analog does fit into region L_2 of the BzR binding site. Illustrated in Figure 7 is the fit of the new ligand **6** and the 7,8-dichloro analog **44** (agonist, 3.6 nM) into the previously developed pharmacophore/receptor model. As clearly illustrated in Figure 7, the lipophilic boundary of the receptor protein readily accepts **44** (X = F, 3.6 nM) but barely permits the binding of **6** [compare **3** (X = H, >1000 nM) to **6** (X = F, 55 nM)]; consequently, the depth of L_2 is certainly close to that defined by the rigid ring of **6**. Substitution of a phenyl group for a chlorine atom at position 7 of diazepam results in ligand **51**, which elicits only weak activity at the BzR. In contrast, the ligand **50** substituted with an ethylene moiety at position 7 binds to the BzR *in vitro* at 24 nM. The lack of affinity of **51** as compared to **50** can be attributed to the inability of region L_2 to accept the large phenyl ring of **51**. This is entirely consistent with the volume of L_2 defined by molecular yardstick **6**.

As mentioned above, the benzo-fused rings at C(8) and C(9) of **1** and **4** interacted with region S_1 and exhibited poor affinity at the BzR [IC_{50}(s) <1000 and 260 nM, respectively]. The 7,9-dichloro-1,4-benzodiazepine **48** (Ro 20-8065) is a full agonist and exhibits an activity comparable to diazepam (see Table 2). From this correlation, it is clear that region L_2 can tolerate a chlorine atom or methyl group at C(9) but not the large benzene ring of **4** which extends into region S_1. The 6,7-benzo-fused ring in **2** and **5** (IC_{50} >1000 nM) extends into the region S_2 illustrated as the boundary between lipophilic regions L_2 and L_3 (see Figure 6). In agreement with this, 1,4-benzodiazepines which bear substituents at position 6 (**52**, **53**) do not exhibit high affinities at the BzR compared to the 6(H)-substituted congeners (Figure 8).[28]

A logical extension of this "molecular yardsticks" approach is the use of (*o*-dimethyl-substituted benzene)- or naphthalene-substituted 1,4-benzodiazepines to probe the dimensions (depth) of the lipophilic regions of the receptor site (see Figure 5 for details). The distance from the center of the benzene (A) ring (L_1) of the 1,4-benzodiazepine nucleus to the end of the fused benzene ring differs from the distance to the terminus of the methyl groups (4.499 Å) or to the end of the fused naphthalene ring (8.224 Å), as illustrated in Figure 5.[27] Once the *in vitro* affinities of a number of these "molecular yardsticks" have been determined, these values can be employed with computer-aided molecular graphics to determine the exact dimensions of lipophilic pockets L_2 and L_3 by simple difference methods. Correlation of the occupation of these pockets with *in vivo* activity can then be made in order to design agents more selective for anxiolytic activity.

The two different pharmacophore/receptor models illustrated in Figures 1 and 2 are important with regard to agonist and inverse agonist activity, respectively, *in vivo* at BzR. Since *in vitro* binding data employed for this work was determined on rat cortical membranes, the potencies likely represent the weighted average of several $GABA_A$ receptor isoforms. The agonist pharmacophore illustrated in Figure 2 represents an inclusive pharmacophore of "diazepam-sensitive" (DS) sites which is clearly different from that of the "diazepam-insensitive" (DI) receptor/model (the major isoform of DI receptors contains an α_6 subunit) reported earlier from this laboratory.[42] The subtle topological differences (i.e., L_2, L_3, S_1, S_2, etc.) between DS $GABA_A$ receptor subtypes can be determined when enough ligands are developed with high selectivity for a specific isoform. Within this context, both the stoichiometry and composition of native receptors must also be evinced. At this juncture it will be possible to subtract (via modeling) the volume of ligands of different isoforms from the inclusive model in order to discover the topological differences between the various $GABA_A$ receptor isoforms. Ligands with rigid rings related to **6**, as well as molecular yardsticks similar to those in Figure 5

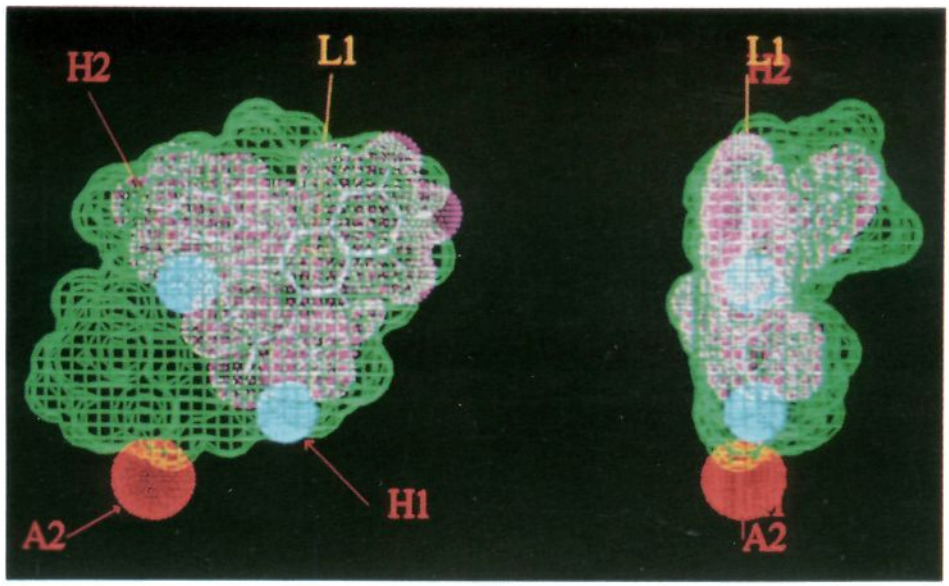

Figure 7. The 7,8-benzo-fused benzodiazepine (**6**) and the dichlorobenzodiazepine (**44**) fitted into the agonist pharmacophore. The magenta dotted areas represent the van der Waals radii of **6**.

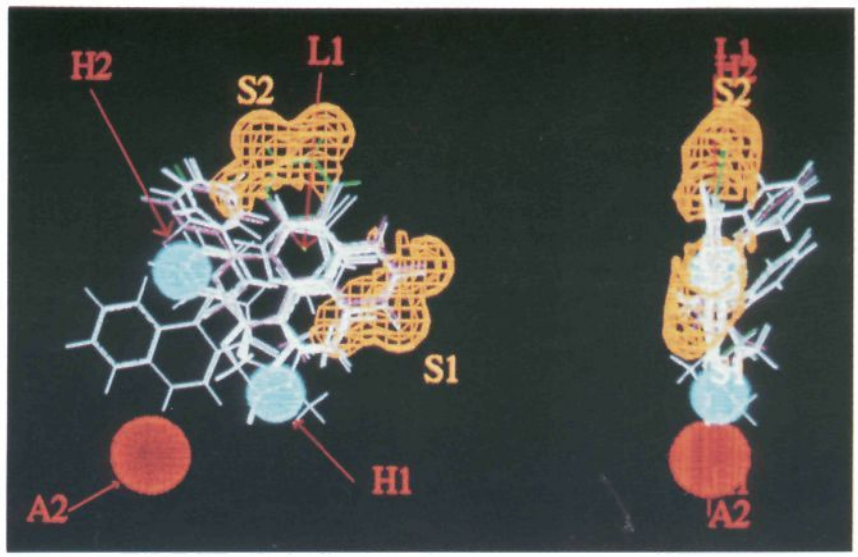

Figure 8. Superposition of the agonists diazepam, Ro-05-4435, brotizolam, etizolam, midazolam, CGS-9896, and **6** with the negative controls **4** (magenta), and **5** (green). The regions of S_1 and S_2 (orange) were derived from subtraction of the union of the positive volumes of diazepam, Ro-05-4435, brotizolam, midazolam, CGS-9896, and **6** from the union of the negative control volumes of **4** and **5**.

(see also footnotes 27 and 37), may be important in determining the differences between native BzR subtypes. Such studies are underway and will be reported in due course.

Experimental Section

In Vitro. The potencies of test compounds to displace [^{3}H]flunitrazepam from benzodiazepine receptors were determined through a modification of previously described procedures.[19,21,24] In brief, rats were killed by decapitation, and the cerebral cortex was removed. Tissues were disrupted in 100 volumes of Tris-citrate buffer (50 mM, pH 7.4) using a Brinkman Polytron (15 s, setting 6). Tissues were centrifuged for 20 min (4 °C) at 20000*g*. The supernatant was discarded and the tissue pellet resuspended in an equal volume of buffer. This "washing" procedure was repeated three times. Tissues were either used fresh or stored at −70 °C until used. Incubations (0.5 mL) consisted of tissue suspension (0.1 mL, ~0.1 mg of protein), 0.05 mL of NaCl solution (2.5 M), 0.05 mL of [^{3}H]flunitrazepam (final concentration, ~1 nM, sp. act. 83.4 Ci/mmol), and drugs and/or buffer to equal volume of Ro 15-1788 (final concentration 10 μM). Incubations (0–4 °C) were initiated by addition of radioligand and teminated after 60 min by rapid filtration under vacuum through GF/B filters with two 5-mL washes of ice-cold buffer. IC_{50} values were estimated using InPlot 4.0 (GraphPAD, San Diego, CA) with at least six concentrations of inhibitor. Values represent $X \pm$ SEM of at least three determinations. Compounds with potencies >1000 nM were generally only tested twice.

In Vivo. Adult male NIH/Swiss mice (25–30 g) were injected intraperitoneally (ip) with graded doses of the compounds (0.1 mL; diluted Emulphor/saline, 1.9) or an equal volume of vehicle (0.1 mL, diluted Emulphor/saline, 1.9). Groups of three to eight mice were injected in graded doses and 12 min later were suspended by their forepaws on a 1.5-mm-thick wire 60 cm above the bench top to assess muscle relaxation; three falls in <1 min was positive for muscle relaxation. At 15 min postinjection mice were injected with PTZ (80 mg/kg) to assess anticonvulsant activity or (40 mg/kg) to assess the proconvulsant activity. Groups of three to eight mice were injected ip with three or four graded doses of drug or vehicle, followed 10 min later by administration of diazepam (2.5 mg/kg ip). After 5 min, the animals were injected

with PTZ (80 mg/kg) to assess the antagonist activity. In vehicle treated mice, 80 mg/kg PTZ produced tonic and clonic convulsions in 100% of the animals, while the incidence of seizes at 40 mg/kg was ~10%. The dose of diazepam (2.5 mg/kg) protected 100% of the mice from PTZ-induced convulsions and also produced muscle relaxation in 100% of the animals tested.

Molecular Modeling. These studies were performed on an Evans & Sutherland PS390 graphics workstation and a Silicon Graphics Personal Iris 4D/35 workstation using SYBYL version 5.5 (Tripos Associates, St. Louis, MO). The starting geometries of the ligands were taken either from X-ray crystallographic structures[13,39-42] or generated using CONCORD.[43] All bond lengths and valence angles of these structures were fully optimized with Gaussian 90[44] or 92[45] *ab initio* calculations (Gaussian Inc., Carnegie-Mellon University, Pittsburgh, PA) at the 3-21G level on a Cray X-MP supercomputer or IBM RS-6000 Model 560 workstation. Substituent groups were then added to the parent compounds to generate the remaining analogs using SYBYL. For example, geometries of 1–6 were arrived at by fusing a rigid benzene ring to diazepam. The side chains were optimized (holding the heterocyclic core structures fixed) using MacroModel BatchMin version 3.5 (Columbia University, New York, NY).[46] Cartessian coordinates for these structures are deposited in the supplementary material of previous publications from this laboratory[42,47] or the present work. Calculations of ring centroids, least-squares fitting, and included volume analyses[48] were also carried out using SYBYL. The lengths of hydrogen-bond extension vectors (HBV) were set to 1.84 Å, while the C–N–HBV and C=O–HBV valence angles used were set to 120 and 135°, respectively, to mimic the geometry of an ideal hydrogen bond.[49-56] The receptor modeling strategy employed here has been applied earlier for the inverse agonist/antagonist and agonist pharmacophores.[19,20]

Materials. Melting points were taken on a Thomas-Hoover melting point apparatus or an Electrothermal Model IA8100 digital melting point apparatus and are reported uncorrected. Proton and carbon NMR spectra were recorded on a Bruker 250-MHz multiple-probe instrument (62.9 MHz for carbon) or a GE 500-MHz spectrometer. Infrared spectra were recorded on a Nicolet Dx FTIR DX V5.07 spectrometer or a Mattson Polaris IR-10400 instrument. Low-resolution mass spectral data (EI/CI) were obtained on a Hewlett-Packard 5985 B GC–mass spectrometer, while high-resolution mass spectral data were obtained on a Finnigan HR mass spectrometer. Microanalyses were performed on a Perkin-Elmer 240C carbon, hydrogen, and nitrogen analyzer. Analytical TLC plates employed were E. Merck Brinkman UV active silica gel (Kieselgel 60 F254) on plastic, and silica gel 60b for flash chromatography was purchased from E. M. Laboratories. All chemicals were purchased from Aldrich Chemical Co. unless otherwise stated. All reactions were carried out under an atmosphere of nitrogen.

1-Amino-2-naphthalenecarbonitrile (**12**),[30] 2-amino-1-naphthalenecarbonitrile (**13**),[30] 2-[(ethoxycarbonyl)amino]naphthalene-1-carbonitrile (**33**),[35] and 3-(dicyanomethylene)-3,4-dihydro-1*H*-naphth[2,1-*d*][1,3]oxazin-1-one (**34**)[35] were prepared according to the method of Tomioka *et al.*[30,35] The spectral properties of these compounds were identical to the reported values.[30,35]

1-Amino-2-benzoylnaphthalene (7) (Procedure a). A solution of 1-amino-2-naphthalenecarbonitrile (**12**) (1 g, 6 mmol) in dry ethyl ether (20 mL) was added to PhMgBr (18 mmol) in dry ethyl ether (100 mL) [which had been prepared from bromobenzene (2.83 g, 18 mmol) and magnesium (0.5 g, 20 mmol)]. The solution was heated to reflux for 1 h, and then aqueous 2 N HCl (100 mL) was added. The mixture was stirred at 30 °C for 2 h. After the solution was neutralized with aqueous NaOH (10%), the ether layer was separated and the water layer was extracted with ether (2 × 100 mL). The ether layer was washed with water and dried (Na_2SO_4). The ether layer was concentrated under reduced pressure, and the residue was purified by flash chromatography (silica gel) with $CHCl_3$ to provide **7**. The solid was recrystallized from CH_3OH to furnish **7** as yellow crystals (1.27 g, 85%): mp 111–112 °C; IR (KBr) 3430, 3402 (NH_2), 1595 (C=O), 1539, 1496, 1307, 1243, 751 cm^{-1}; ^1H NMR (DMSO-d_6) δ 6.92 (d, 1H, J = 9 Hz), 7.28 (d, 1H, J = 9 Hz), 7.48–7.56 (m, 6H), 7.61 (t, 1H, J = 8 Hz), 7.75 (d, 1H, J = 8 Hz), 8.44 (d, 1H, J = 8 Hz), 8.61 (br s, 2H, NH_2); ^{13}C NMR ($CDCl_3$) δ 199.1 (s, C=O), 150.1 (s), 140.9 (d), 136.1 (d), 131.0 (s), 130.0 (d), 129.1 (s), 128.9 (d), 128.5 (d), 128.1 (s), 125.4 (d), 123.1 (s), 121.7 (d), 114.8 (s), 111.3 (d); MS (EI) m/e 247 (M^+, 74), 246 (100), 217 (6), 170 (15), 115 (21). Anal. ($C_{17}H_{13}NO$) C, H, N.

1-Benzoyl-2-aminonaphthalene (8). 2-Amino-12-naphthalenecarbonitrile (**13**) (3.6 g, 21 mmol) was treated as described in procedure a, although the hydrolysis required heating with aqueous 6 N HCl for 5 h. The solid was purified by flash chromatography (silica gel) with hexane/ethyl acetate (4:1) to provide **8** as yellow crystals (4.5 g, 86%): mp 169–170 °C; IR (KBr) 3431, 3283 (NH_2), 3056, 1597 (C=O), 1542, 1461, 1247, 783, 703 cm^{-1}; ^1H NMR (DMSO-d_6) δ 5.89 (br s, 2H, NH_2), 7.02–7.17 (m, 4H), 7.45 (t, 2H, J = 7.6 Hz), 7.56–7.64 (m, 3H), 7.68–7.72 (m, 1H), 7.76 (d, 1H, J = 8.9 Hz); ^{13}C NMR ($CDCl_3$) δ 198.97 (s, C=O), 145.40 (s), 139.58 (s), 132.85 (d), 132.91 (s), 132.58 (d), 129.70 (d), 128.57 (d), 128.13 (d), 127.32 (s), 126.66 (d), 125.21 (d), 122.43 (d), 118.87 (d), 114.56 (s); MS (EI) m/e 247 (M^+, 100). Anal. ($C_{17}H_{13}NO$) C, H, N.

2-Amino-3-benzoylnaphthalene (9). 3-Amino-2-naphthoic acid (**14**) (1 g, 5.35 mmol) was dissolved in dry THF (50 mL), and phenyllithium (11 mL of 2.5 M, 21.4 mmol) was added into the solution at 0 °C. The mixture was then stirred for 2 h at 25 °C. Aqueous saturated NH_4Cl solution (20 mL) was added to the mixture, after which the THF layer was separated and the water layer was extracted with ether (2 × 50 mL). The THF and ether extracts were combined and purified by flash chromatography with hexane/EtOAc (6:1) to provide **9** (0.61 g, 51%) and diphenyl 2-(3-aminonaphthyl)]methanol (**15**) (0.18 g, 10% yield). **9**: light yellow crystals; mp 119–120 °C (CH_3OH); IR (KBr) 3477, 3371 (NH), 1643 (C=O), 1630, 1571, 890, 759 cm^{-1}; ^1H NMR (DMSO-d_6) δ 6.33 (br s, 2H, NH_2), 7.08 (s, 1H), 7.10 (t, 1H, J = 7.4 Hz), 7.39 (t, 1H, J = 7.4 Hz), 7.53–7.59 (m, 3H), 7.64–7.72 (m, 4H), 7.89 (s, 1H); MS (EI) m/e 247 (M^+, 43), 246 (47), 230 (4), 217 (9), 170 (10), 142 (17), 115 (100). Anal. ($C_{17}H_{13}NO$) C, H, N.

15: mp 160–161 °C (hexane/EtOAc); IR (KBr) 3449 (OH), 3386, 3354 (NH), 3053, 1635, 1610, 1455, 769, 701 (cm^{-1}); ^1H NMR (DMSO-d_6) δ 5.38 (br s, 2H, D_2O exchangeable, NH_2), 6.77 (s, 1H), 6.90 (s, 1H), 7.00 (dt, 1H, J = 1, 7.0 Hz), 7.03 (s, 1H, D_2O exchangeable, OH), 7.36–7.20 (m, 11H), 7.49 (d, 1H, J = 8.15 Hz); MS (EI) m/e 325 (M^+, 14), 306 (100), 276 (2), 246 (4), 230 (31), 202 (6), 115 (29), 105 (23).

2-Phenyl-4*H*-naphth[2,3-*d*][1,3]oxazin-4-one (23) (Procedure b). 3-Amino-2-naphthoic acid (**14**) (3 g, 17.8 mmol) was dissolved in benzoyl chloride (50 mL), and the mixture was heated to 170 °C for 3 h. The mixture was then cooled to room temperature, whereupon crystals formed. The solid was collected and washed with hexane/ether (2:1) to give **23** (3.8 g, 91%) as colorless crystals: mp 227–228 °C; IR(KBr) 1753 (C=O), 1611, 1282, 1170, 751, cm^{-1}; ^1H NMR ($CDCl_3$) δ 7.48–7.70 (m, 5H), 7.98 (d, 1H, J = 8.5 Hz), 8.03 (d, 1H, J = 8.5 Hz), 8.15 (s, 1H), 8.32–8.36 (m, 2H), 8.87 (s, 1H); MS(CI) m/e 274 ($M^+ + 1$, 100). Anal. ($C_{18}H_{11}NO_2$) C, H, N.

2-(2′-Fluorobenzoyl)-3-(*N*-benzoylamino)naphthalene (24) (Procedure c). A solution of 2-bromofluorobenzene (1.54 g, 8.82 mmol) in dry THF (20 mL) was cooled to −78 °C, and *n*-BuLi (6.1 mL of 1.6 M, 9.7 mmol) was added dropwise to the solution. After the mixture was stirred for 15 min at −78 °C, it was transferred into a solution of 2-phenylnaphth[2,3-*d*]oxazin-4-one **23** (2.5 g, 9.1 mmol) in dry THF (250 mL) which was precooled to −78 °C. The mixture was then stirred at −78 °C for 20 min. Aqueous saturated NH_4Cl solution (50 mL) was added to the reaction mixture, and it was warmed to room temperature. The organic layer was separated, washed with water, and dried ($MgSO_4$). After the THF was removed under reduced pressure, the residue was purified by flash chromatography with hexane/ethyl acetate (95:5) to provide **24** (1.71 g, 51%) and bis(2′-fluorophenyl)[3-(*N*-benzoylamino)-2-naphthyl]methanol (**25**) (0.6 g, 14%). **24**: mp 188–189 °C (hexane/EtOAc); IR (KBr) 3298 (NH), 3056, 1681, 1633, 1546, 1303, 757 (cm^{-1}); ^1H NMR ($CDCl_3$) δ 7.24 (t, 1H, J = 8.5 Hz), 7.31 (dt, 1H, J = 1, 8 Hz), 7.41 (dt, 1H, J = 1, 8 Hz), 7.46–7.61 (m, 6H), 7.72 (d, 1H, J = 8.2 Hz), 7.90 (d, 1H, J = 8.2 Hz), 8.12–8.15 (m, 3H), 9.40 (s, 1H), 12.12 (br s, 1H, NH); ^{19}F NMR ($CDCl_3$) δ (CF_3CO_2H, external −41.30 (s); MS (EI) m/e 369 (M^+, 23), 264 (1.5), 246 (20), 105 (100). Anal. ($C_{24}H_{16}FNO_2$) C, H, N.

25: mp 210–211 °C (hexane/EtOAc); IR (KBr) 3395 (OH),

3234 (NH), 3043, 1638 (C=O), 1546, 1384, 855, 702 cm^{-1}; ^{1}H NMR ($CDCl_3$) δ 4.49 (t, 1H, J = 7.8 Hz), 7.02–7.30 (m, 7H), 7.31–7.52 (m, 10H), 7.88 (d, 1H, J = 8.3 Hz), 9.01 (s, 1H), 10.2 (br s, 1H); MS (CI) m/e 467 (M^+ + 1, 35), 466 (M^+, 27), 449 (100).

2-Amino-3-(2′-fluorobenzoyl)naphthalene (26) (Procedure d). The (*N*-benzoylamino)naphthalene **24** (1 g, 3.77 mmol) was dissolved in glacial acetic acid (50 mL), and 48% HBr (25 mL) was added to the solution. The mixture was heated to reflux for 10 h, after which the solvent was removed under reduced pressure. The residue was then dissolved in EtOAc (50 mL) and washed with aqueous $NaHCO_3$ solution (5%) followed by water and then dried ($MgSO_4$). After the EtOAc was removed under reduced pressure, the residue was purified by a wash column which was eluted with hexane/EtOAc (3:1) to afford **26** (0.73 g, 97%) as yellow crystals: mp 108–109 °C; IR (KBr) 3483, 3372 (NH), 3062, 1628 (C=O), 1605, 1308, 765 cm^{-1}; ^{1}H NMR (DMSO-d_6) δ 6.12 (br s, 2H, NH_2), 7.24 (s, 1H), 7.35–7.48 (m, 3H), 7.52 (dt, 1H, J = 1, 6.6 Hz), 7.65 (dt, 1H, J = 1, 6.6 Hz), 7.72–7.82 (m, 4H), 8.17 (d, 1H, J = 2 Hz); ^{19}F NMR ($CDCl_3$) δ (CF_3CO_2H, external) −42.19 (s); MS (EI) m/e 265 (M^+, 84), 264 (52), 245 (32), 170 (16), 142 (23), 115 (100). Anal. ($C_{17}H_{12}FNO$) C, H, N.

1-Amino-2-naphthoic Acid (29). 1-Amino-2-cyanonaphthalene (**12**) (5 g, 30 mmol) was dissolved in ethanol (150 mL), and aqueous 20% NaOH solution (50 mL) was added. The mixture was heated to reflux for 10 h. After the ethanol was removed under reduced pressure, the aqueous solution was brought to pH 6.5 with aqueous concentrated HCl to furnish a white precipitate. The solid was collected, washed with water, and dried under vacuum to provide **29** (4.2 g, 85%): mp 270 °C [(dec) lit.[57] mp: 198–199 °C]; IR (KBr) 3161, 3156, 3018, 2896, 2867, 2792 ($RCO_2^-RNH_3^+$), 1677 (C=O), 1617, 1442 cm^{-1}; ^{1}H NMR (DMSO-d_6) δ 7.66–7.77 (m, 2H), 7.86 (d, 1H, J = 8.7 Hz), 8.01 (d, 2H, J = 8.7 Hz), 8.90 (d, 1H, J = 7.4 Hz); MS (EI) m/e 187 (M^+, 16), 141 (19).

2-Phenyl-4*H*-naphth[1,2-*d*][1,3]oxazin-4-one (30). 1-Amino-2-naphthoic acid (**29**) (4.2 g 22 mmol) was reacted with benzoyl chloride under conditions analogous to that described in procedure b to provide the title compound **30** as a white solid (5.87 g, 91%): mp 192–193 °C; IR (KBr) 3055, 1754 (C=O), 1607, 1567, 758, 700 cm^{-1}; ^{1}H NMR ($CDCl_3$) δ 7.64 (m, 3H), 7.65–7.80 (m, 2H), 7.82–8.00 (m, 2H), 8.13 (d, 1H, J = 8.7 Hz), 8.45 (m, 2H), 9.06 (m, 1H); MS (EI) m/e 273 (M^+, 59), 245 (2), 229 (13), 196 (17), 140 (9), 126 (23), 105 (100). Anal. ($C_{18}H_{11}NO_2$) C, H, N.

1-(*N*-Benzoylamino)-2-(2′-fluorobenzoyl)naphthalene (31). The 2-phenylnaphth[1,2-*d*]oxazin-4-one **30** (3.5 g, 12.8 mmol) was treated under conditions analogous to those of procedure c to provide **31** (4.1 g, 85%) as bright yellow crystals (hexane/EtOAc): mp 169–170 °C; IR (KBr) 3278 (NH), 3070, 1661 (C=O), 1610, 1517, 1302, 1101, 837, 758 cm^{-1}; ^{1}H NMR ($CDCl_3$) δ 7.06–7.23 (m, 2H), 7.40–7.65 (m, 8H), 7.73 (d, 1H, J = 8 Hz), 7.86 (dd, 1H, J = 1, 8 Hz), 7.95–8.10 (m, 3H), 10.03 (br s, 1H); MS (EI) m/e 369 (M^+, 7), 264 (2), 246 (33), 235 (3), 140 (2), 105 (100). Anal. ($C_{24}H_{16}FNO_2$) C, H, N.

1-Amino-2-(2′-fluorobenzoyl)naphthalene (32). 1-(*N*-Benzoylamino)-2-(2′-fluorobenzoyl)naphthalene (**31**) (3.05 g, 8.3 mmol) was treated according to procedure d to afford **32** (2.2g, 95%) as light green-yellow crystals: mp 119–121 °C; IR (KBr) 3499, 3377 (NH_2), 3058, 1612 (C=O), 1520, 1483, 913, 815, 741 cm^{-1}; ^{1}H NMR ($CDCl_3$) δ 6.94 (d, 1H, J = 8.3 Hz), 7.11–7.30 (m, 3H), 7.41–7.51 (m, 3H), 7.57 (dt, 1H, J = 1.2, 8.1 Hz), 7.70 (br s, 2H, NH_2), 7.71 (dd, 1 H, J = 1.2, 8.3 Hz), 7.96 (d, 1H, J = 8.4 Hz); MS (EI) m/e 265 (M^+, 91), 264 (87), 246 (30), 170 (36), 115 (100). Anal. ($C_{17}H_{12}FNO$) C, H, N.

1-(2′-Fluorobenzoyl)-2-aminonaphthalene (36). 3-(Dicyanomethylene)-3,4-dihydro-1*H*-naphth[2,1-*d*][1,3]oxazin-1-one (**34**) (1.3 g, 5 mmol) was treated as described in procedure c with 2 equiv of (*o*-fluorophenyl)lithium, and this was followed by treatment analogous to procedure d to afford **36** (0.93 g, 71%) as light brown crystals (hexane/EtOAc): mp 98–99 °C; ^{1}H NMR ($CDCl_3$) δ 5.60 (br s, 2H, NH_2), 6.90 (d, 1H, J = 9 Hz), 6.98–7.17 (m, 4H), 7.17–7.40 (m, 2H), 7.26 (d, 1H, J = 9 Hz), 7.62 (dd, 1H, J = 1.5, 9 Hz), 7.72 (d, 1H, J = 9 Hz); IR (KBr) 3494, 3381 (NH_2), 3064, 1645, 1620, 1602 (C=O), 818, 747 cm^{-1}; MS (EI) m/e 265 (M^+, 100), 264 (71), 248 (20), 246 (25), 170 (75), 142 (30), 115 (90). Anal. ($C_{17}H_{12}FNO$) C, H, N.

General Procedure e To Prepare Bromoacetyl Amides. 1-[*N*-(Bromoacetyl)amino]-2-benzoylnaphthalene (16). 1-Amino-2-benzoylnaphthalene (**7**) (0.7 g, 2.8 mmol) and $NaHCO_3$ (1 g, 11 mmol) were suspended in dry $CHCl_3$ (50 mL), and a solution of bromoacetyl bromide (0.63 g, 3.1 mmol) in dry $CHCl_3$ (10 mL) was added dropwise at 0 °C. The mixture was stirred at 0 °C for 30 min. The $CHCl_3$ solution was washed with aqueous $NaHCO_3$ solution (2%) and dried ($MgSO_4$). After the $CHCl_3$ was removed under reduced pressure, the oily residue was purified by a wash column on silica gel [hexane/EtOAc (4:1)] to provide **16** as colorless crystals (1.03 g, 94%): mp 199–201 °C; IR (KBr) 3268 (NH), 3015, 1665 (C=O), 1525, 814 cm^{-1}; ^{1}H NMR ($CDCl_3$) δ 3.93 (s, 2H), 7.42–7.49 (m, 3H), 7.26–7.56 (m, 3H), 7.77–7.93 (m, 5H), 9.30 (br s, 1H, NH); MS (EI) m/e 369 (M^+, 18), 367 (M^+, 18), 264 (26), 246 (100), 217 (38), 105 (37). Anal. ($C_{18}H_{14}BrNO$) C, H, N.

2-[*N*-(Bromoacetyl)amino]-1-benzoylnaphthalene (18). 2-Amino-1-benzoylnaphthalene (**8**) (2.6 g, 10.5 mmol) was treated as described in procedure e to provide **18** as yellow needles (3.4 g, 89%): mp 157–158 °C; IR (KBr) 3241 (NH), 3063, 1673 (C=O), 1583, 1539 (C=O), 828 cm^{-1}; ^{1}H NMR (DMSO-d_6) δ 3.79 (s, 2H), 7.46–7.48 (m, 4H), 7.53 (m, 1H), 7.61–7.66 (m, 4H), 8.02 (d, 1H, J = 8.5 H), 8.10 (d, 1H, J = 8.5 Hz), 10.19 (br s, 1H); MS (EI) m/e 369 (M^+, 39), 367 (M^+, 40), 264 (97), 262 (100), 246 (72), 217 (64), 183 (77), 105 (56). Anal. ($C_{19}H_{14}BrNO$) C, H, N.

2-[*N*-(Bromoacetyl)amino]-3-benzoylnaphthalene (21). 2-Amino-3-benzoylnaphthalene (**9**) (1.2 g, 4.9 mmol) was treated as described in procedure e to provide **21** as light yellow crystals (1.7 g, 94%): mp 145–146 °C; IR (KBr) 3241 (NH), 3062, 1670 (C=O), 1637 (C=O), 1537, 761 cm^{-1}; ^{1}H NMR ($CDCl_3$) δ 4.07 (s, 2H), 7.69–7.38 (m, 5H), 7.70–7.85 (m, 3H), 7.78 (d, 1H, J = 8.5 Hz), 8.11 (s, 1H), 9.01 (s, 1H), 11.31 (br s, 1H, NH); MS (EI) m/e 369 (M^+, 34), 367 (M^+, 34), 246 (68), 217 (89), 105 (100). Anal. ($C_{19}H_{14}BrNO$) C, H, N.

1-[*N*-(Bromoacetyl)amino]-2-(2′-fluorobenzoyl)naphthalene (37). 1-Amino-2-(2′-fluorobenzoyl)naphthalene (**32**) (2.2 g, 8.3 mmol) was treated as described in procedure e to provide **37** as colorless crystals (2.95 g, 92%): mp 169–172 °C; IR (KBr) 3281 (NH), 3069, 1669 (C=O), 1650, 1606, 1519, 756 cm^{-1}; ^{1}H NMR ($CDCl_3$) δ 3.96 (s, 2H), 7.14 (dt, 1H, J = 0.7, 9.4 Hz), 7.25 (dt, 1H, J = 0.8, 7.6 Hz), 7.64–7.48 (m, 4H), 7.67 (dt, 1H, J = 0.8, 7.6 Hz), 7.80 (d, 1H, J = 8.6 Hz), 7.88 (m, 1H), 7.97 (m, 1H), 9.55 (br s, 1H, NH); MS (EI) m/e 387 (M^+, 16), 385 (M^+, 16), 292 (6), 264 (68), 246 (14), 183 (20), 140 (23), 123 (100), 115 (27). Anal. ($C_{19}H_{13}BrFN_2O$) C, H, N.

2-[*N*-(Bromoacetyl)amino]-1-(2′-fluorobenzoyl)naphthalene (39). 2-Amino-1-(2′-fluorobenzoyl)naphthalene (**36**) (0.73 g, 2.8 mmol) was treated as described in procedure e to provide **39** as colorless crystals (0.98 g, 92%): mp 139–141 °C; IR (KBr) 3281 (NH), 3057, 1650 (C=O), 1556, 1362, 825, 743 cm^{-1}; ^{1}H NMR ($CDCl_3$) δ 3.99 (s, 2H), 7.08 (t, 1H, J = 8 Hz), 7.16 (t, 1H, J = 7.8 Hz), 7.20–7.55 (m, 4H), 7.63 (t, 1H, J = 7.8 Hz), 7.97 (d, 1H, J = 8.1 Hz), 8.24 (d, 1H, J = 8.1 Hz), 9.51 (br s, 1H, NH); MS (EI) m/e 387 (M^+, 20), 385 (M^+, 21), 264 (100), 235 (28), 183 (63), 123 (59), 115 (24). Anal. ($C_{19}H_{13}BrFN_2O$) C, H, N.

2-[*N*-(Bromoacetyl)amino]-3-(2′-fluorobenzoyl)naphthalene (41). 2-Amino-3-(2′-fluorobenzoyl)naphthalene (**26**) (0.39 g, 1.1 mmol) was treated as described in procedure e to provide **41** as colorless crystals (0.295 g, 90%): mp 181–182 °C (hexane/EtOAc); IR (KBr) 3208 (NH), 1665 (C=O), 1641, 1533, 1300, 760 (cm^{-1}); ^{1}H NMR ($CDCl_3$) δ 4.01 (s, 2H), 7.21 (m, 1H), 7.31 (dt, 1H, J = 1.1, 7.1 Hz), 7.42 (dt, 1H, J = 1.1, 6.9 Hz), 7.63–7.53 (m, 3H), 7.72 (d, 1H, J = 8.2 Hz), 7.87 (d, 1H, J = 8.2 Hz), 8.08 (d, 1H, J = 2.3 Hz), 9.11 (s, 1H), 11.58 (br s, 1H, NH); MS (EI) m/e 387 (M^+, 62), 385 (M^+, 62), 292 (13), 264 (62), 246 (12), 235 (31), 196 (14), 123 (100). Anal. ($C_{19}H_{13}BrFN_2O$) C, H, N.

General Procedure f for Amination followed by Cyclization To Prepare the Benzo-Fused 1,4-Benzodiazepines. 5-Phenyl-1,3-dihydronaphtho[1,2-*e*][1,4]diazepin-2-one (17). The bromoacetyl amide **16** (0.11 g, 0.3 mmol) was dissolved in a saturated solution of ammonia in CH_3OH (150 mL) and the mixture was heated to reflux for 10 h. After the methanol was removed under reduced pressure, the solid which remained was purified by a wash column (silica gel) eluted with hexane/EtOAc (3:1). The purified material was recrystallized from $CHCl_3/CH_3OH$ to provide the benzo-fused benzodiazepine **17** (0.078 g, 74%)

as colorless crystals: mp 245–246 °C dec; IR (KBr) 3212 (NH), 3078, 1658 (C=O), 1363, 821, 751 cm^{-1}; ^{1}H NMR (DMSO-d_6) δ 3.79 (d, 1H, J = 9.8 Hz), 4.58 (d, 1H, J = 9.8 Hz), 7.23 (d, 1H, J = 8.6 Hz), 7.40–7.54 (m, 5H), 7.66–7.72 (m, 3H), 7.99 (m, 1H), 8.36 (m, 1H); ^{13}C NMR (DMSO-d_6) δ 169.79, 138.92, 135.92, 134.25, 130.19, 129.27, 128.28, 128.25, 126.93, 126.31, 125.71, 123.89, 123.71, 123.43, 57.23; MS (EI) m/e 286 (M$^+$, 12), 257 (86), 230 (100), 140 (62); MS(CI) m/e 287 (M$^+$, 89). Anal. ($C_{19}H_{14}N_2O$) C, H, N.

5-Phenyl-1,3-dihydronaphtho[2,1-*e*][1,4]diazepin-2-one (19). The *N*-(bromoacetyl)-1-benzoyl-2-naphthylamine 18 (3.2 g, 8.7 mmol) was treated as described in procedure f to provide 19 as colorless crystals (0.97 g, 39%) accompanied by 2-hydroxy-3-amino-4-phenylbenzo[*f*]quinoline 20 (1.09 g, 44%). 19: mp 259–259.8 °C (hexane/EtOAc); IR (KBr) 3213 (NH), 3056, 1681 (C=O), 1625, 1606, 1364, 744 cm^{-1}; ^{1}H NMR (DMSO-d_6) δ 3.89 (d, 1H, J = 10 Hz), 4.56 (d, 1H, J = 10 Hz), 7.23–7.44 (m, 9H), 7.93 (d, 1H, J = 9 Hz), 8.09 (d, 1H, J = 9 Hz), 10.76 (br s, 1H); ^{13}C NMR (DMSO-d_6) δ 170.85, 168.47, 140.19, 138.56, 131.99, 131.03, 129.81, 120.70, 128.36, 128.28, 128.19, 127.07, 126.60, 125.05, 120.57, 57.51; MS (EI) m/e 286 (M$^+$, 100), 285 (37), 257 (60), 230 (29), 183 (50), 155 (23). Anal. ($C_{19}H_{14}N_2O$) C, H, N.

20: mp 328 °C dec; IR (KBr) 3465, 3375, 3110, 3050, 1655 (C=O), 1570, 808 cm^{-1}; ^{1}H NMR (DMSO-d_6) δ 4.67 (br s, 2H, NH_2), 6.93 (m, 1H), 7.06 (d, 1H, J = 8.7 Hz), 7.27 (t, 1H, J = 6.8 Hz), 7.32 (m, 2H), 7.48–7.76 (m, 4H), 7.70 (d, 1H, J = 8.8 Hz), 7.80 (d, 1H, J = 7.8 Hz), 10.46 (br s, 1H, NH); ^{13}C NMR (DMSO-d_6) δ 156.54 (s), 138.74 (s), 135.54 (s), 130.66 (s), 130.25 (s), 130.09 (d), 129.09 (d), 128.75 (d), 128.66 (s), 127.97 (d), 126.27 (d), 124.92 (d), 124.77 (d), 123.65 (d), 120.36 (d), 116.75 (d), 114.13 (s); MS (EI) m/e 286 (M$^+$, 100), 267 (13), 255 (12), 240 (30), 202 (16), 120 (10).

5-Phenyl-1,3-dihydronaphtho[2,3-*e*][1,4]diazepin-2-one (22). The bromoacetyl amide 21 (0.52 g, 1.4 mmol) was treated as described in procedure f to provide 22 (0.35 g, 78%) as colorless crystals: mp 271–274 °C; IR (KBr) 3194 (NH), 3050, 2975, 1682 (C=O), 1632, 1607, 882 cm^{-1}; ^{1}H NMR ($CDCl_3$) δ 4.37 (s, 2H), 7.32–7.51 (m, 4H), 7.52–7.63 (m, 4H), 7.75 (d, 1H, J = 10 Hz), 7.83 (d, 1H, J = 6.7 Hz), 7.85 (s, 1H), 8.87 (br s, 1H, NH); ^{13}C NMR ($CDCl_3$) δ 171.39 (s), 169.76 (s), 139.52 (s), 136.40 (s), 133.92 (s), 131.16 (d), 130.22 (d), 129.24 (d), 128.58 (d), 128.29 (d), 128.19 (d), 126.75 (d), 126.35 (s), 125.71 (d), 117.46 (d), 56.60 (dd); MS (EI) m/e 286 (M$^+$, 24), 258 (37), 257 (36), 230 (37), 202 (35), 140 (100), 127 (96). Anal. ($C_{19}H_{14}N_2O$) C, H, N.

5-(2-Fluorophenyl)-1,3-dihydronaphtho[1,2-*e*][1,4]diazepin-2-one (38). *N*-(Bromoacetyl)-2-(2′-fluorobenzoyl)naphthylamine (37) (3.2 g, 8.3 mmol) was treated as described in procedure f to provide 38 as colorless crystals (2 g, 80%): mp 255–256 °C, ^{1}H NMR (DMSO-d_6) δ 4.44 (br s, 2H), 7.05 (dt, 1H, J = 0.8, 9.4 Hz), 7.23 (t, 1H, J = 6.6 Hz), 7.42 (m, 1H), 7.50–7.70 (m, 4H), 7.88 (dd, 1H, J = 2.5, 6.9 Hz), 8.22 (dd, 1H, J = 2.2, 7.1 Hz), 9.24 (br s, 1H, NH); MS (EI) m/e 304 (M$^+$, 100), 275 (88), 200 (30), 154 (32), 137 (38), 127 (79), 114 (48). Anal. ($C_{19}H_{13}FN_2O$) C, H, N.

5-(2-Fluorophenyl)-1,3-Dihydronaphtho[2,1-*e*][1,4]diazepin-2-one (40). The *N*-(bromoacetyl)-1-(2′-fluorobenzoyl)-2-naphthylamine (39) (0.7 g, 1.8 mmol) was treated as described in procedure f to provide 40 as colorless crystals (0.495 g, 90%): mp 259 °C dec; IR (KBr) 3200 (NH), 1680 (C=O), 1625, 1600, 1445, 1350, 750 cm^{-1}; ^{1}H NMR ($CDCl_3$) δ 4.00 (d, 1H, J = 10.3 Hz), 4.94 (dd, 1H, J = 1.8, 10.3 Hz), 6.85 (m, 1H), 7.16 (dt, 1H, J = 0.9, 7.5 Hz), 7.20–7.40 (m, 4H), 7.44 (d, 1H, J = 8.5 Hz), 7.62 (dt, 1H, J = 1.6, 7.5 Hz), 7.82 (d, 1H, J = 8.1 Hz), 7.94 (d, 1H, J = 8.8 Hz), 9.02 (br s, 1H); MS (EI) m/e 304 (M$^+$, 100), 284 (22), 258 (11), 255 (14), 142 (11), 114 (17). Anal. ($C_{19}H_{13}FN_2O$) C, H, N.

5-(2-Fluorophenyl)-1,3-dihydronaphtho[2,3-*e*][1,4]diazepin-2-one (42). *N*-(bromoacetyl)-3-(2′-fluorobenzoyl)-2-naphthylamine (41) (0.21 g, 5.4 mmol) was treated as described in procedure f to provide 42 as colorless crystals (0.14 g, 85%): mp 263 °C dec; IR (KBr) 3200 (NH), 1675 (C=O), 1625, 1440, 755 cm^{-1}; ^{1}H NMR ($CDCl_3$) δ 4.41 (s, 2H), 7.02 (m, 1H), 7.25 (dt, 1H, J = 1.1, 8.5 Hz), 7.40–7.51 (m, 2H), 7.54 (m, 1H), 7.53 (s, 1H), 7.64 (dt, 1H, J = 1, 8.5 Hz), 7.72 (d, 1H, J = 8.8 Hz), 7.74 (s, 1H), 7.77 (d, 1H, J = 8.8 Hz), 8.43 (br s, 1H, NH); ^{13}C NMR ($CDCl_3$) δ 172.33 (s), 167.98 (s), 160.57 (d, J_{CF} = 252 Hz), 134.49 (s), 134.40 (s), 131.90 (dd, J_{CCCCF} = 8.1 Hz), 131.43 (d), 130.74 (d), 129.46 (s), 128.55 (d), 128.34 (s), 127.72 (s), 127.05 (d), 126.22 (d), 124.26 (dd, J_{CCCF} = 3 Hz), 117.99 (d), 116.23 (dd, J_{CCF} = 22 Hz), 56.35 (t); MS (EI) m/e 304 (M$^+$, 100), 285 (18), 276 (87), 248 (19), 220 (10), 127 (28). Anal. ($C_{19}H_{13}FN_2O$) C, H, N.

General Procedure g for N-Methylation of the 1,4-Benzodiazepines. 1-Methyl-5-phenyl-1,3-dihydro-naphtho-[1,2-*e*][1,4]diazepin-2-one (1). The 8,9-benzo-fused 1,4-benzodiazepine 17 (0.51 g, 1.78 mmol) was dissolved in dry DMF (40 mL), and NaH (46 mg, 1.92 mmol) was added to the solution in small portions. After the mixture which resulted was stirred at 25 °C for 10 min, CH_3I (0.27 g, 1.95 mmol) was added and the slurry was stirred for 30 min. The DMF was then removed under reduced pressure. The residue was purified by flash chromatography [hexane/ethyl acetate (10:1)] to provide the title compound 1 (0.485 g, 87%) as colorless crystals: mp 165–167 °C; IR (KBr) 3057, 1670 (C=O), 1599, 1650, 832 cm^{-1}; ^{1}H NMR ($CDCl_3$) δ 3.44 (s, 3H), 3.84 (d, 1H, J = 10.2 Hz), 4.88 (d, 1H, J = 10.2 Hz), 7.31 (d, 1H, J = 8.6 Hz), 7.39–7.48 (m, 3H), 7.62–7.72 (m, 5H), 7.92 (m, 1H), 8.01 (m, 1H); MS (EI) m/e 300 (M$^+$, 74), 299 (72), 272 (100), 255 (8), 229 (5), 165 (8). Anal. ($C_{20}H_{16}N_2O \cdot {}^1/_3H_2O$) C, H, N.

1-Methyl-5-phenyl-1,3-dihydronaphtho[2,1-*e*][1,4]diazepin-2-one (2). The 6,7-benzo-fused 1,4-benzodiazepine 19 (0.6 g, 2.1 mmol) was treated as described in procedure g to provide 2 (0.564 g, 90%) as colorless crystals: mp 188–189 °C; IR (KBr) 3063, 2988, 1688 (C=O), 1606, 1506, 988, 750 (cm^{-1}); ^{1}H NMR (DMSO-d_6) δ 3.39 (s, 3H), 3.90 (d, 1H, J = 10.3 Hz), 4.62 (d, 1H, J = 10.3 Hz), 7.24–7.40 (m, 8H), 7.75 (d, 1H, J = 9.0 Hz), 8.00 (d, 1H, J = 8.1 Hz), 8.20 (d, 1H, J = 9 Hz); ^{13}C NMR (DMSO-d_6) δ 170.13 (s), 168.26 (s), 141.98 (s), 139.80 (s), 132.01 (d), 130.26 (s), 130.13 (d), 128.58 (d), 128.36 (d), 128.12 (d), 127.12 (d), 126.92 (s), 125.79 (d), 122.95 (s), 120.31 (d), 57.25 (dd), 34.14 (q); MS (EI) m/e 300 (M$^+$, 100), 299 (35), 272 (76), 255 (15), 197 (46), 182 (8). Anal. ($C_{20}H_{16}N_2O$) C, H, N.

1-Methyl-5-phenyl-1,3-dihydronaphtho[2,3-*e*][1,4]diazepin-2-one (3). The 7,8-benzo-fused 1,4-benzodiazepine 22 (0.22 g, 0.77 mmol) was treated as described in procedure g to provide 3 as colorless crystals (0.2g, 87%): mp 167.5–168.7 °C; IR (KBr) 3058, 2857, 1671 (C=O), 1634, 1608, 893, 730 cm^{-1}; ^{1}H NMR (DMSO-d_6) δ 3.51 (s, 3H, NCH_3), 3.86 (d, 1H, J = 10.8 Hz), 4.76 (d, 1H, J = 10.8 Hz), 7.35–7.51 (m, 4H), 7.58 (t, 1H, J = 7.7 Hz), 7.63–7.68 (m, 2H), 7.73 (s, 1H), 7.75 (d, 1H, J = 8.4 Hz), 7.81 (s, 1H), 7.86 (d, 1H, J = 8.4 Hz); ^{13}C NMR ($CDCl_3$) δ 171.29 (s), 170.43 (s), 141.31 (s), 139.36 (s), 134.22 (s), 131.0 (d), 130.47 (d), 129.65 (d), 129.25 (s), 128.49 (d), 128.29 (d), 128.01 (s), 127.30 (d), 126.55 (d), 118.55 (d), 56.80 (dd), 35.44 (q); MS (EI) m/e 300 (M$^+$, 36), 299 (32), 272 (54), 255 (27), 202 (43), 127 (100). Anal. ($C_{20}H_{16}N_2O$) C, H, N.

1-Methyl-5-(2′-fluorophenyl)-1,3-dihydronaphtho[1,2-*e*]-[1,4]diazepin-2-one (4). The 8,9-benzo-fused 1,4-benzodiazepine 38 (0.6 g, 2 mmol) was treated as described in procedure g to provide 4 (0.543 g, 91%) as colorless crystals: mp 178–180 °C; IR (KBr) 3062, 2931, 1681 (C=O), 1613, 1588, 1450, 763 cm^{-1}; ^{1}H NMR ($CDCl_3$) δ 3.43 (s, 3H), 3.86 (d, 1H, J = 10.5 Hz), 4.93 (d, 1H, J = 10.5 Hz), 7.05 (m, 1H), 7.18 (dd, 1H, J = 0.6, 8 Hz), 7.26 (dt, 1H, J = 1, 8 Hz), 7.45 (m, 1H), 7.56–7.70 (m, 2H), 7.72 (dt, 1H, J = 1, 8 Hz), 7.89 (m, 1H), 8.00 (m, 2H); MS (EI) m/e 318 (M$^+$, 86), 317 (87), 299 (37), 290 (100), 168 (19), 145 (29), 127 (47). Anal. ($C_{20}H_{15}FN_2O$) C, H, N.

1-Methyl-5-(2′-fluorophenyl)-1,3-dihydronaphtho[2,1-*e*]-[1,4]diazepin-2-one (5). The 6,7-benzo-fused 1,4-benzodiazepine 40 (0.13 g, 0.5 mmol) was treated as described in procedure g to provide 5 (0.122 g, 91%) as colorless crystals: mp 145–147 °C; IR (KBr) 3075, 2994, 1675 (C=O), 1606, 1513, 819, 750 cm^{-1}; ^{1}H NMR ($CDCl_3$) δ 3.49 (s, 3H), 3.93 (d, 1H, J = 10.3 Hz), 4.90 (d, 1H, J = 10.3 Hz), 6.85 (ddd, 1H, J = 1, 7.2, 10.8 Hz), 7.20 (dt, 1H, J = 1.2, 7.6 Hz), 7.25 (dt, 1H, J = 1.4, 7.7 Hz), 7.30–7.50 (m, 4H), 7.60 (dt, 1H, J = 1.9, 7.7 Hz), 7.82 (d, 1H, J = 9.0 Hz), 7.79 (d, 1H, J = 9.0 Hz); MS (EI) m/e 318 (M$^+$, 100), 299 (18), 290 (70), 269 (11), 197 (83), 168 (55), 127 (55). Anal. ($C_{20}H_{15}FN_2O$) C, H, N.

1-Methyl-5-(2′-fluorophenyl)-1,3-dihydronaphtho[2,3-*e*]-[1,4]diazepine-2-one (6). The 7,8-benzo-fused 1,4-benzodiazepine 42 (0.11 g, 0.35 mmol) was treated as described in procedure g to provide 6 (0.105 g, 91%) as colorless crystals: mp 136–137

°C (hexane/EtOAc); IR (KBr) 1676 (C=O), 1635, 1612, 1445, 1317, 750 cm^{-1}; ^{1}H NMR ($CDCl_3$) δ 3.52 (s, 3H), 3.88 (d, 1H, J = 10.7 Hz), 4.80 (d, 1H, J = 10.7 Hz), 7.01 (ddd, 1H, J = 1, 2, 9.3 Hz), 7.24 (dt, 1H, J = 1.1, 7.6 Hz), 7.38–7.50 (m, 2H), 7.55 (dt, 1H, J = 1.3, 7.7 Hz), 7.71 (s, 1H), 7.71 (m, 2H), 7.72 (s, 1H), 7.84 (d, 1H, J = 8.4 Hz); ^{13}C NMR ($CDCl_3$) δ 170.82 (s), 167.52 (s), 160.00 (d, J_{CF} = 252 Hz), 140.22 (s), 134.28 (s), 132.04 (dd, J_{CCCF} = 7 Hz), 131.38 (d), 129.21 (d), 128.48 (d), 127.36 (d), 126.54 (d), 124.38 (dd, J_{CCCCF} = 3 Hz), 118.87 (d), 116.24 (dd, J_{CCF} = 21 Hz), 56.77 (dd), 35.61 (q); MS (EI) m/e 318 (M^+, 100), 299 (27), 290 (89), 275 (13), 262 (7), 233 (13), 127 (25). Anal. ($C_{20}H_{16}FN_2O$) C, H, N.

Attempted Conversion of (Fluorobenzoyl)naphthalene 24 into (Fluorobenzoyl)aminonaphthalene 26. 2-(2′-Fluorobenzoyl)-3-(*N*-benzoylamino)naphthalene (24) (100 mg, 0.27 mmol) was dissolved in ethanol (30 mL), and 5% NaOH solution was added. The mixture was heated to reflux for 2 h. After the ethanol was removed under reduced pressure, the aqueous solution was extracted with $CHCl_3$ (20 mL × 3) and dried over $MgSO_4$. After the $CHCl_3$ was removed under reduced pressure, the residue was purified by a wash column which was eluted with hexane/EtOAc (3:1) to afford benz[*b*]acridin-12(5*H*)-one[58] (28) as light brown crystals (57 mg, 86%): mp 298 °C dec (lit.[58] mp 303 °C); IR (KBr) 3257 (NH), 1050, 1640, 1627, 1590 (C=O), 1335, 1104, 743 cm^{-1}; ^{1}H NMR (DMSO-d_6) δ 7.20 (dt, 1H, J = 1.9, 7.8 Hz), 7.42 (dt, 1H, J = 1.9, 7.9 Hz), 7.52 (d, 1H, J = 8.3 Hz), 7.59 (dt, 1H, J = 2, 7.8 Hz), 7.74 (dt, 1H, J = 2, 7.9 Hz), 7.93 (s, 1H), 7.99 (d, J = 8.4 Hz), 8.15 (d, 1H, J = 8.3 Hz), 8.24 (d, 1H, J = 8.1 Hz), 8.92 (s, 1H), 11.2 (br s, NH); MS (EI) m/e 245 (M^+, 100), 216 (31), 189 (20), 140 (12).

Attempted Conversion of Aminonaphthalenecarbonitrile 12 and Amino Acid 14 into (Fluorobenzoyl)aminonaphthalene 26. A solution of 2-bromofluorobenzene (1.5 g, 8.8 mmol) in dry THF (30 mL) was cooled to −78 °C and *n*-BuLi (6 mL of 1.6 M, 9.6 mmol) was added dropwise to the solution. After the mixture was stirred for 20 min at −78 °C, a solution of naphthylnitrile 12 (0.54 g, 2.8 mmol) or 14 (individually) in 50 mL THF was added. After the mixture had been stirred for 5 h at −78 °C, the solution was stirred at −50 °C for three h (in both cases, the reaction was monitored by TLC and only starting material was observed). When the temperature was raised to −30 °C, the light yellow solution turned to brown. The reaction was then quenched with aq. saturated NH_4Cl solution (30 mL). The reaction mixture was worked up to provide starting 12 or 14 accompanied by biphenylene (213 mg) mp 112–114 °C (lit. 113–114)[59]; ^{1}H NMR ($CDCl_3$) δ 7.65 (dd, 4H, J = 2.8, 6.2 Hz), 8.65 (dd, 4H, J = 2.8, 6.2 Hz); MS(EI) m/e 152 (M^+, 100).

Supplementary Material Available: The *ab initio* optimized coordinates, connection tables, and Mulliken charges for the benzo-fused 1,4-benzodiazepines (1–3) and the parent 1-methyl-5-phenyl-1,4-benzodiazepin-2-one (3 pages). Ordering information given on any current masthead page.

Acknowledgment. We wish to thank the NIMH (MH46851) for generous financial support of this work.

References

(1) Tyrer, P. The Benzodiazepine Bonanza. *Lancet* 1974, September 21, 709–710.
(2) Squires, R. *GABA and Benzodiazepine Receptors*; CRC Press: Boca Raton, FL, 1988; Vols. 1 and 2.
(3) Olsen, R. W.; Tobin, A. J. Molecular biology of $GABA_A$ receptors. *FASEB J.* 1990, *4*, 1469–80.
(4) Wisden, W.; Laurie, D. J.; Monyer, H.; Seeburg, P. H. The distribution of 13 $GABA_A$ receptor subunit mRNAs in the rat brain. I. Telencephalon, diencephalon, mesencephalon. *J. Neurosci.* 1992, *12*, 1040–1062.
(5) Levitan, E. S.; Schofield, P. R.; Burt, D. R.; Rhee, L. M.; Wisden, W.; Kohler, M.; Fujita, N.; Rodriguez, H. F.; Stephenson, F. A.; Darlison, M.; Barnard, E. A.; Seeburg, P. H. Structural and functional basis for $GABA_A$ receptor heterogeneity. *Nature (London)* 1988, *335*, 76–79.
(6) Burt, D.; Kamatchi, G. $GABA_A$ receptor subtypes: from pharmacology to molecular biology. *FASEB J.* 1991, *5*, 2916–2923.
(7) Pritchtt, D.; Luddens, H.; Seeburg, P. Type I and Type II $GABA_A$-benzodiazepine receptors produced in transfected cells. *Science* 1989, *245*, 1389–1392.
(8) Wong, G.; Sei, Y.; Skolnick, P. Stable expression of type I γ-aminobutyric $acid_A$/benzodiazepine receptors in a transfected cell line. *Mol. Pharm.* 1992, *42*, 996–1005.
(9) Skolnick, P.; Wong, G. Drug-receptor interactions in anxiety. In *Imidazopyridines in Anxiety Disorders: A Novel Experimental and Therapeutic Approach*; Bartholini, G., Garreau, M., Morselli, P., Zivkovic, B., Eds.; Raven Press: New York, 1993; pp 23–32.
(10) Villar, H. O.; Davies, M. F.; Loew, G. H.; Maguire, P. A. Molecular models for recognition and activation at the benzodiazepine receptor: a review. *Life Sci.* 1991, *48*, 593–602.
(11) Crippen, G. M. Distance geometry analysis of the benzodiazepine binding site. *Mol. Pharmacol.* 1982, *22*, 11–19.
(12) (a) Fryer, R. I. Ligand interactions at the benzodiazepine receptor. In *Comprehensive Medicinal Chemistry*; Emmett, J., Ed.; Pergamon Press Inc.: Oxford, U.K., 1989; Vol. 3, pp 539–566. (b) Fryer, R. I.; Gu, Z. Q.; Wang, C. G. Synthesis of novel substituted 4*H*-imidazo[1,5-*a*][1,4]-benzodiazepines. *J. Heterocycl. Chem.* 1991, *28*, 1661–1669.
(13) Codding, P. W.; Muir, A. K. S. Molecular structure of Ro15-1788 and a model for the binding of benzodiazepine receptor ligands. *Mol. Pharmacol.* 1985, *28*, 178–184.
(14) Allen, M. S.; Hagen, T. J.; Trudell, M. L.; Codding, P. W.; Skolnick, P.; Cook, J. M. Synthesis of novel 3-substituted β-carbolines as benzodiazepine receptor ligands: probing the benzodiazepine receptor pharmacophore. *J. Med. Chem.* 1988, *31*, 1854–1861.
(15) Borea, P. A.; Gilli, G.; Bertolasi, V.; Ferretti, V. Stereochemical features controlling binding and intrinsic activity properties of benzodiazepine-receptor ligands. *Mol. Pharmacol.* 1987, *31*, 334–344.
(16) Tebib, S.; Bourguignon, J. J.; Wermuth, C. G. The active analog approach applied to the pharmacophore identification of benzodiazepine receptor ligands. *J. Comput-Aided Mol. Design* 1987, *1*, 153–170.
(17) Villar, H. O.; Uyeno, E. T.; Toll, L.; Polgar, W.; Davies, M. F.; Loew, G. H., Molecular determination of benzodiazepine receptor affinities and anticonvulsant activities. *Mol. Pharmacol.* 1989, *36*, 586–600.
(18) Trudell, M. L.; Lifer, S. L.; Tan Y.-C.; Martin, M. J.; Deng, L.; Skolnick, P.; Cook, J. M. Synthesis of substituted 7,12-dihydropyrido[3,2-*b*:5,4-*b*′]diindoles: rigid planar benzodiazepine receptor ligands with inverse agonist/antagonist properties. *J. Med. Chem.* 1990, *33*, 2412–2420.
(19) Allen, M. S.; Tan, Y.-C.; Trudell, M. L.; Narayanan, K.; Schindler, L. R.; Martin, M. J.; Schultz, C.; Hagen, T. J.; Koehler, K. F.; Codding, P. W.; Skolnick, P.; Cook, J. M. Synthesis and computer-assisted analysis of the pharmacophore for the benzodiazepine receptor inverse agonist site. *J. Med. Chem.* 1990, *33*, 2343–2357.
(20) Diaz-Arauzo, H.; Koehler, K.; Hagen, T. J.; Cook, J. M. Synthetic and computer assisted analysis of the pharmacophore for agonists at benzodiazepine receptors. *Life Sci.* 1991, *49*, 207–216.
(21) Diaz-Arauzo, H.; Evoniuk, G. E.; Skolnick, P.; Cook, J. M. The agonist pharmacophore of the benzodiazepine receptor. Synthesis of a selective anticonvulsant/anxiolytic. *J. Med. Chem.* 1991, *34*, 1754–1756.
(22) Skolnick, P.; Schweri, M.; Kutter, E.; Williams, E.; Paul, S. M. Inhibition of [^{3}H]diazepam and [^{3}H]3-carboethoxy-β-carboline binding by irazepine: evidence for multiple "domains" of the benzodiazepine receptor. *J. Neurochem.* 1982, *39*, 1142–1146.
(23) Skolnick, P.; Paul, S. New concepts in the neurobiology of anxiety. *J. Clin. Psychiatry* 1983, *44*, 12–20.
(24) Martin, M. J.; Trudell, M. L.; Allen, M. S.; Díaz-Araúzo, H.; Deng, L.; Schultz, C. A.; Tan, Y.-C.; Bi, Y.; Narayanan, K.; Dorn, L. J.; Koehler, K. F.; Skolnick, P.; Cook, J. M. Molecular yardsticks. Rigid probes to define the spatial dimensions of the benzodiazepine receptor binding site. *J. Med. Chem.* 1992, *35*, 4105–4117.
(25) Hollinshead, S. P.; Trudell, M. L.; Skolnick, P.; Cook, J. M. Structural requirements for agonist actions at the benzodiazepine receptor: studies with analogues of 6-(benzyloxy)-4-(methoxymethyl)-β-carboline-3-carboxylic acid ethyl ester. *J. Med. Chem.* 1990, *33*, 1062–1069.
(26) Narayanan, C.; Cook, J. M. Molecular yardsticks: synthesis of higher homologs of 7,12-dihydropyrido[3,4-*b*:5,4-*b*′]diindole. Probing the dimensions of the benzodiazepine receptor inverse agonist site. *Heterocycles* 1990, *31*, 203–209.
(27) Comparison of the *in vitro* affinities of the 7,8-bis(trihalo) analogs (CCl_3 vs CBr_3 vs CI_3) will define the dimensions of the cleft in the orthogonal direction as well, resulting in the total receptor volume of the lipophilic pockets. Occupation of these pockets can then be correlated with *in vivo* activity (full vs partial spectrum).

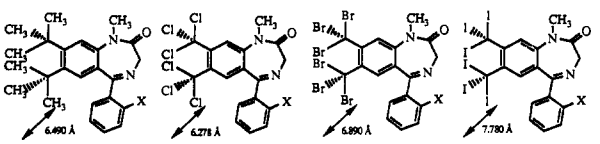

Three-dimensional molecular yardsticks to measure the volume of a receptor pocket in definite increments. The distances pictured are the van der Waals field range in the direction orthogonal to the plane of the paper.

(28) Haefely, W.; Kyburz, E.; Gereche, M.; Mohler, H. P. Recent advances in the molecular pharmacology of benzodiazepine receptors and in the structure-activity relationships of their agonists and antagonists. *Adv. Drug Res.* **1985**, *14*, 165–322.
(29) The synthesis of the intermediates (**7**, **8**, **9**, **26**, **32**, and **36**) have been reported in preliminary form. Zhang, W.; Liu, R.; Cook, J. M. The regiospecific synthesis of ortho aminonaphthophenones via the addition of carbanions to naphthoxazin-4-ones. *Heterocycles* **1993**, *36*, 2229–2236.
(30) Tomioka, Y.; Ohkubo, K.; Yamazaki, M. Studies on aromatic nitro compounds. V. A simple one-pot preparation of *o*-aminoarylnitriles from some aromatic nitro compounds. *Chem. Pharm. Bull.* **1985**, *33*, 1360–1366.
(31) Clemence, F.; Le Martret, O.; Collard, J. New route to N-aryl and N-heteroaryl derivatives of 4-hydroxy-3-quinoline carboxamides. *J. Heterocycl. Chem.* **1984**, *21*, 1345–1353.
(32) Hino, K.; Kawashima, K.; Oka, M.; Nagai, Y.; Uno, H.; Matsumoto, J. A novel class of antiulcer agents. 4-Phenyl-2-(1-piperazinyl)-quinolines. *Chem. Pharm. Bull.* **1989**, *37*, 110–115.
(33) Aristoff, P. A.; Johnson, P. D.; Harrison, A. W. Total synthesis of a novel antiulcer agent via a modification of the intramolecular Wadsworth-Emmons-Wittig reaction. *J. Am. Chem. Soc.* **1985**, *107*, 7967–7974.
(34) Heilbron, I. *Dictionary of Organic Compounds*; Pollock, J. R. A., Stevens, R., Eds.; Oxford University Press: New York, 1965; Vol. 4, pp 168.
(35) Ohshima, T.; Tomioka, Y.; Yamazaki, M. Studies on aromatic nitro compounds. II. Reaction of 2-nitronaphthalene with malononitrile in the presence of base. *Chem. Pharm. Bull.* **1981**, *29*, 1292–1298.
(36) Sternbach, L. H. 1,4-Benzodiazepines. Chemistry and some aspects of the structure activity relation. *Angew. Chem., Int. Ed. Engl.* **1971**, *10*, 34–43.
(37) The IC_{50} values of a number of pyridodiindoles and pyridoimidazoles are currently being employed to define the exact location of S_2. See ref 24 for details.

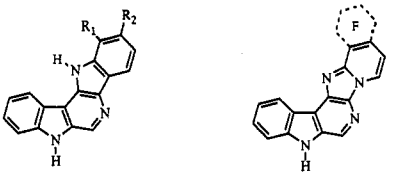

4 nM. $R_1 = R_2 = H$ a
83 nM. $R_1 = CH_3$, $R_2 = H$
8 nM. $R_1 = H$, $R_2 = CH_3$
560 nM. $R_1 = R_2 = CH_3$ b

39 nM, ligand devoid of ring F; c
>1,000 nM, ring F=phenyl

(a) See ref 18; (b) Petro, M.; Skolnick, P.; Cook, J. M. Unpublished results; (c) See ref 24.
(38) Klopman, G.; Contreras, R. Use of artificial intelligence in the structure-activity correlation of anticonvulsant drugs. *Mol. Pharmacol.* **1985**, *27*, 86–93.
(39) Camerman, A.; Camerman, N. Stereochemical basis of anticonvulsant drug action. II. Molecular structure of diazepam. *J. Am. Chem. Soc.* **1972**, *94*, 268–272.
(40) Hempel, A.; Camerman, N.; Camerman, A. Benzodiazepine stereochemistry: crystal structures of the diazepam antagonist Ro 15-1788 and the anomalous benzodiazepine Ro 5-4864. *Can. J. Chem.* **1987**, *65*, 1608–1612.
(41) Neidle, S.; Webster, G. D.; Jones, G. B.; Thurston, D. E. Structures of two DNA minor-groove binders, based on pyrrolo[2,1-*c*][1,4]-benzodiazepines. *Acta Crystallogr.* **1991**, *C47*, 2678–2680.
(42) Wong, G.; Koehler, K. F.; Skolnick, P.; Gu, Z.-Q.; Ananthan, S.; Schonholzer, P.; Hunkeler, W.; Zhang, W.; Cook, J. M. Synthetic and computer assisted analysis of the structural requirements for selective, high affinity ligand binding to 'diazepam-insensitive' benzodiazepine receptors. *J. Med. Chem.* **1993**, *36*, 1820–30.
(43) Pearlman, R. S.; Balducci, R.; McGarity, C.; Rusinko, A. III; Skell, J. CONCORD. **1990**, University of Texas, Austin, TX.
(44) Frisch, M. J.; Head-Gordon, M.; Trucks, G. W.; Foresman, J. B.; Schlegel, H. B.; Raghavachari, K.; Robb, M. A.; Binkley, J. S.; Gonzalez, C.; Defrees, D. J.; Fox, D. J.; Whiteside, R. A.; Seeger, R.; Melius, C. F.; Baker, J.; Martin, L. R.; Kahn, L. R.; Stewart, J. J. P.; Topiol, S.; Pople, J. A. *Gaussian 90*; Gaussian, Inc.: Pittsburgh, PA, 1990.
(45) Frisch, M. J.; Trucks, G. W.; Head-Gordon, M.; Gill, P. M. W.; Wong, M. W.; Foresman, J. B.; Johnson, B. G.; Schlegel, H. B.; Robb, M. A.; Replogle, E. S.; Gomperts, R.; Anderes, J. L.; Raghavachari, K.; Binkley, J. S.; Gonzalez, C.; Martin, L. R.; Fox, D. J.; Defrees, D. J.; Baker, J.; Stewart, J. J. P.; Pople, J. A. *Gaussian 92, Revision A*; Gaussian, Inc.: Pittsburgh, PA, 1992.
(46) Mohamadi, F.; Richards, N. G. J.; Guida, W. C.; Liskamp, R.; Caufield, C.; Chang, G.; Hendrickson, T.; Still, W. C. MacroModel-An integrated software system for modeling organic and bioorganic molecules using molecular mechanics. *J. Comput. Chem.* **1990**, *11*, 440–467.
(47) Allen, M. S.; LaLoggia, A. J.; Dorn, L. J.; Martin, M. J.; Costantino, G.; Hagen, T. J.; Koehler, K. F.; Skolnick, P.; Cook, J. M. Predictive binding of β-carboline inverse agonists and antagonists via the CoMFA/GOPLE approach. *J. Med. Chem.* **1992**, *35*, 4001–4010.
(48) Sufrin, J. R.; Dunn, D. A.; Marshall, G. R. Steric mapping of the L-methionine binding site of ATP: L-methionine S-adenosyltransferase. *Mol. Pharmacol.* **1981**, *19*, 307–313.
(49) Boobbyer, D. N.; Goodford, P. J.; McWhinnie, P. M.; Wade, R. C. New hydrogen-bond potentials for use in determining energetically favorable binding sites on molecules of known structure. *J. Med. Chem.* **1989**, *32*, 1083–94.
(50) Ippolito, J. A.; Alexander, R. S.; Christianson, D. W. Hydrogen bond stereochemistry in protein structure and function. *J. Mol. Biol.* **1990**, *215*, 457–71.
(51) Murray,-Rust, P.; Glusker, J. P. Directional hydrogen bonding to sp2 and sp3-hybridized oxygen atoms and its relevance to ligand-macromolecular interactions. *J. Am. Chem. Soc.* **1984**, *106*, 1018–1025.
(52) Thanki, N.; Thornton, J. M.; Goodfellow, J. M. Distributions of water around amino acid residues in proteins. *J. Mol. Biol.* **1988**, *202*, 637–57.
(53) Tintelnot, M.; Andrews, P. Geometries of functional group interactions in enzyme-ligand complexes: guides for receptor modelling. *J. Comput.-Aided Molec. Des.* **1989**, *3*, 67–84.
(54) Vedani, A.; Dunitz, J. D. Lone-pair directionality in H-bond potential functions for molecular mechanics calculations. *J. Am. Chem. Soc.* **1985**, *107*, 7653–7658.
(55) Vedani, A.; Hutha, D. W. An algorithm for the systematic solvation of proteins based on the directionality of hydrogen bonds. *J. Am. Chem. Soc.* **1990**, *112*, 4759–4767.
(56) Vedani, A.; Huhta, D. W. A new force field for modeling metalloproteins. *J. Am. Chem. Soc.* **1991**, *113*, 5860–5862.
(57) (a) Ferbenind, I. G., Ger. Pat. 622 308, Nov 25, 1935; *Chem. Abst.* 1911, *33*, 949. (b) Reddy, M. S.; Ratnam, C. V. Synthesis of new heterocycles: condensation of 2-methyl-4H-naphth[1,2-d][1,3]oxazin-4-one with Schiff bases and formation of 3-aryl-2-styrylbenzo[h]quinazolin-4(3H)-ones. *Bull. Chem. Soc. Jpn.* **1985**, *58*, 2449–2450.
(58) Narasimhan, N. S.; Ranade, A. C. Synthetic applications of lithiation reactions. II. Syntheses of N-phenylnaphthostyril and 2,3-benzacridone. *Indian J. Chem.* **1969**, *7*, 538–539.
(59) Aldrich Chemical Company, Inc. Catalog, 1993, pp 147.